Green Chemistry

Accepted Manuscript

ROYAL SOCIETY OF CHEMISTRY

www.rsc.org/greenchem

Table of contents entry

Advancements in solid acid catalysts for biodiesel synthesis

Fang Su and Yihang Guo*

Recent advancements in biodiesel synthesis catalyzed by solid acids, particularly novel hybrid organic-inorganic solid acids, are reviewed.

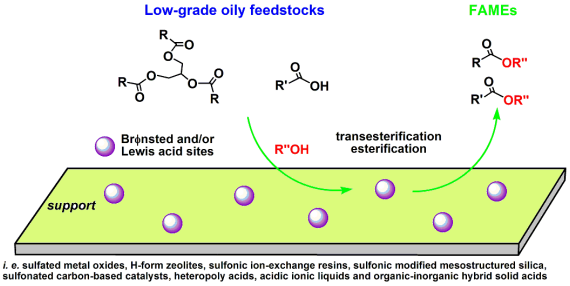

Cite this: DOI: 10.1039/c0xx00000x

www.rsc.org/xxxxxx

ARTICLE TYPE

Advancements in solid acid catalysts for biodiesel production

Fang Su and Yihang Guo*

Received (in XXX, XXX) Xth XXXXXXXXX 20XX, Accepted Xth XXXXXXXXX 20XX
DOI: 10.1039/b000000x

Biodiesel has emerged as one of the most potential renewable energy to replace current petroleum-based diesel. It is a sustainable, biodegradable and non-toxic diesel fuel substitute that can be easily produced through base- or acid-catalyzed esterification and transesterification reactions. The conventional base catalysts, although effective, are limited to use of refined vegetable oils, leading to the process impractical and uneconomical due to high feedstock cost and priority as food resources. Biodiesel production processes based on the use of acid catalysts are good alternatives to conventional processes because of their simplicity and the simultaneous promotion of esterification and transesterification reactions from low-grade, highly-acidic and water-containing oils without soap formation. Highly reactive homogeneous Brønsted acid catalysts are efficient for this process, but they suffer from serious contamination and corrosion problems that make essential the implementation of good separation and purification steps. More recently, a "*green*" approach to biodiesel production has stimulated the application of sustainable solid acid catalysts as replacements for such liquid acid catalysts so that the use of harmful substances and generation of toxic wastes are avoided; meanwhile, the ease of catalyst separation after the reactions can be realized. Recent studies have proved the technical feasibility and the environmental and economical benefits of biodiesel production *via* heterogeneous acid-catalyzed esterification and transesterification. In this perspective, various solid acids including sulfated metal oxides, H-form zeolites, sulfonic ion-exchange resins, sulfonic modified mesostructured silica materials, sulfonated carbon-based catalysts, heteropolyacids and acidic ionic liquids are reviewed as the heterogeneous catalysts in esterification and transesterification. Meanwhile, for the purpose of facilitating mass-transport of solid acid-catalyzed biodiesel production process and improving the catalytic stability of the solid acid catalysts in esterification and transesterification reactions, novel and robust organic-inorganic hybrid acid catalysts with unique advantages including strong Brønsted as well as Lewis acid properties, well-defined mesostructure and enhanced surface hydrophobicity are successfully designed, which have been highlighted in this review.

Fang Su received her BSc degree in chemistry from Langfang Teachers University (China) in 2009. She is currently pursuing her PhD under the supervision of Prof. Yihang Guo at Key Lab of Polyoxometalate Science of Ministry of Education, Northeast Normal University (China). Her research interest focuses on design of heteropolyacid-based hybrid organic-inorganic catalysts with controllable structural orderings and pore geometries and their applications in biodiesel production as well as conversion of biomass-derived platform molecules to value-added chemicals.

Yihang Guo obtained her BSc and PhD degrees from Northeast Normal University (China) in 1985 and 2001. She was a Postdoctoral Fellow at the University of York (UK) in the Green Chemistry Centre of Excellence directed by Prof. James Clark in 2006-2007. She has been a professor at Northeast Normal University since 2001 and her current research interests cover hybrid organic-inorganic porous materials and their applications in biodiesel production and conversion of biomass-derived platform molecules to value-added chemicals and photo functional materials for environment remediation.

1. Introduction

The rapid consumption of finite fossil fuel reserves and the emissions of greenhouse gases (GHG) and associated climate change are driving the development of the alternative and sustainable energy sources derived from renewable feedstocks.[1–8] Oil is the most important source of energy worldwide, accounting for some 35% of primary energy consumption and the majority of the chemical feedstocks; the quest for sustainable resources to meet demands of a constantly rising global population is one of the main challenges for mankind this century.[9] Renewable energy sources such as solar energy, wind energy, hydro energy and energy from biomass and waste (*i.e.* the so-called biofuel including bioethanol and biodiesel) have been successfully developed and used by different nations to limit the use of fossil fuels. Nevertheless, based on recent study from International Energy Agency, only biofuels have the highest potential among renewable resources.[10,11] Biofuels are attractive from a policy perspective for several reasons. In addition to offering the potential for GHG reductions, they may also offer security of fuel supply and a new agricultural product for stimulating rural economies.

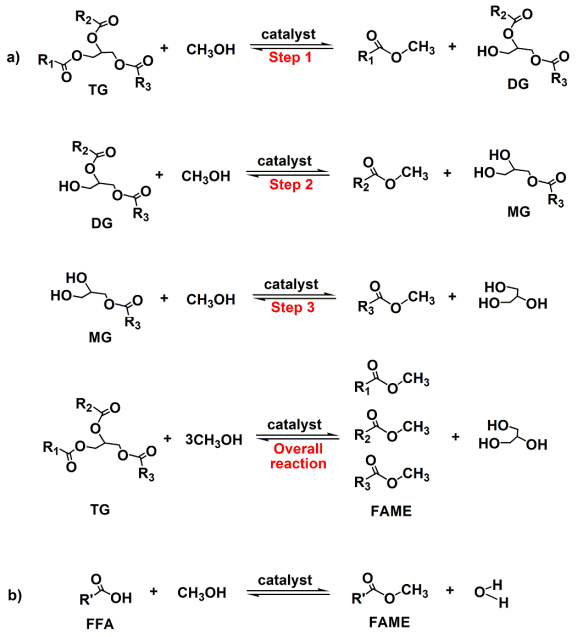

Fig. 1 Acid- or base-catalyzed biodiesel synthesis routes: transesterification of TG (a) and esterification of FFA (b) with methanol.

Biodiesel is a mixture of C_{12}–C_{22} fatty acid monoalkyl esters (FAMEs), and it is a sustainable, sulfur-free, biodegradable and non-toxic diesel fuel substitute that is widely used worldwide.[12–15] Biodiesel has a significant added value compared to petroleum-based diesel, reflected in a series of improved properties including fewer carcinogenic particulate matter emissions, increased lubricity and biodegradability as well as ease of handling, transport and storage.[1] Biodiesel can be easily produced from the transesterification of triglycerides (TGs) in the presence of acid or base catalysts. As illustrated in Fig. 1a, complete transesterification of a TG molecule suffers from three consecutive steps, resulting in diglyceride (DG), monoglyceride (MG) and then FAME. The overall net reaction produces 3 mol of FAME and 1 mol of glycerol for each mole of TG transformed. If free fatty acids (FFAs) exist in the feedstocks, esterification of FFAs with short-chained alcohols (*e.g.* methanol or ethanol) also can produce FAMEs (Fig. 1b). Compared with esterification of FFAs, transesterification of TGs is a more complex process with multiple steps, more intermediates produced as well as higher activation energy, and therefore, the transesterification reaction proceeds at a slower rate. For biodiesel production, a wide range of feedstocks can potentially be employed, and they range from conventional edible oils (*e.g.* palm, rapeseed, sunflower and soybean), used vegetable oils and animal fats to inedible oils from alternative feedstocks (*e.g.* *Jatropha Curcas* oil and *Eruca Sativa Gars* oil). "*First-generation*" biodiesel is derived from edible feedstocks, however, biodiesel production from refined vegetable oils is impractical and uneconomical due to high feedstock cost and priority as food resources. "*Second-generation*" biodiesel is produced from inedible feedstocks, which are competitive for the commercial use of biodiesel production because of their low price and high yield. Nevertheless, these low-grade virgin plant oils generally contain high content of FFAs and water as well as trace salts, which may interfere with biodiesel production process. Therefore, rational design of novel and efficient catalysts for biodiesel production from inedible feedstocks is an important challenge, which is the main focus that will be discussed in this perspective.

2. Current status of biodiesel production

Methods of biodiesel production can be classified as chemical catalytic (base or acid catalysis), biocatalytic (enzyme catalysis) and non-catalytic processes, which have been reviewed by some excellent articles.[1,6] Herein, we only give a brief description concerning about the chemical catalysis for the biodiesel production.

Conventionally, biodiesel is produced using homogeneous strong base catalysts such as alkali metal hydroxides and alkoxides.[16–21] The base-catalyzed transesterification reaction can be carried out at relatively mild temperatures (*e.g.* 50–80 °C), and the rates of reaction are good at relatively low alcohol-to-oil molar ratio (*e.g.* 5: 1).[12] Unfortunately, homogeneous base catalysts suffer from many drawbacks including sensitivity to water and FFA. Both of the components may induce saponification under alkaline conditions (Fig. 2a), which not only

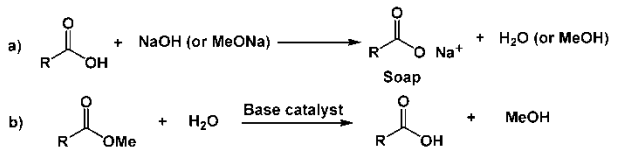

Fig. 2 Esterification of FFA under alkaline conditions to yield soap and water (a); formation of FFA *via* reaction of fatty acid monoalkyl ester with water under alkaline conditions. The process can deactivate the catalyst and form soap again (b).

consumes the catalyst but also causes the formation of emulsions. Accordingly, virgin plant oils like soybean oil, rapeseed oil or palm oil with FFA content less than 0.5% (or acid value less than 1 mg KOH/g), an anhydrous alkali catalyst and anhydrous

alcohol are necessary for commercially viable alkali-catalyzed production systems.[22] This requirement is likely to be a significant limitation to the use of low-cost feedstocks.[8] As a result, biodiesel production by these routes is still not cost-competitive with petrodiesel. In order to overcome the above disadvantages, an acid catalyzed pre-esterification is applied to remove any FFAs before the oil is contacted with the soluble base catalyst.[2] Additionally, solid base catalysts such as base zeolites,[23] alkali earth metal oxides,[19,24–27] hydrotalcites (or layered double hydroxides),[4,28,29] alumina loaded with various compounds[30] and mixed oxide[31] have been quite successful with high conversion and yield of biodiesel obtained. However, the basic sites may be poisoned by strong adsorption of FFA and water on the surface sites. Furthermore, excessive soap in the products can inhibit the subsequent purification process of biodiesel, including glycerol separation and water washing. Apart from that, high water content in some feedstocks can hydrolyze FAMEs to form FFAs (Fig. 2b); meanwhile, the basic active sites in the catalyst will be neutralized by FFAs thus formed and contained in the feedstocks, which prevent biodiesel production by transesterification.[32]

With respect to base catalysts, biodiesel production processes based on the use of acid catalysts are good alternatives to conventional processes because of their simplicity and the simultaneous promotion of esterification and transesterification reactions without soap formation. Thus, the acid catalysts can directly produce biodiesel from low-grade, highly-acidic and water-containing oils. Homogenous acid catalysts including strong Brønsted mineral acids (*e.g.* sulfuric acid or hydrofluoric acid) and *p*-toluenesulfonic acid, although effective, lead to serious contamination and corrosion problems that make essential the implementation of good separation and purification steps.[22,33,34] Therefore, homogeneous acid-catalyzed system is not a popular choice for commercial applications.[35] More recently, a "*green*" approach to biodiesel synthesis has stimulated the application of sustainable solid acid catalysts as replacements for such liquid acid catalysts so that the use of harmful substances and generation of toxic wastes are avoided; meanwhile, the ease of catalyst separation after the reactions can be realized. Recent studies have proved the technical feasibility and the environmental and economical benefits of biodiesel production *via* heterogeneous acid-catalyzed esterification and transesterification.[36,37] To date, various solid acid catalysts including sulfated metal oxides (*e.g.* SO_4^{2-}/ZrO_2, SO_4^{2-}/Ta_2O_5, SO_4^{2-}/Nb_2O_5 and SO_4^{2-}/TiO_2), H-form zeolites, sulfonic ion-exchange resins, sulfonic modified mesostructure silica, sulfonated carbon-based catalyst, heteropolyacids (HPAs) and acidic ionic liquids (ILs) have been studied for biodiesel production. However, owing to serious mass-transport limitation problems, especially for transesterification of TGs in heterogeneous acid-catalyzed systems as well as high viscosity and poor miscibility of feedstocks with light alcohols, the reaction rate of most of the above solid acid-catalyzed biodiesel production is severely hampered. Accordingly, higher temperature, higher pressure, higher alcohol-to-oil molar ratio as well as longer reaction time are required to obtain considerably high FAME yields. These stringent conditions are not favourable for industrial applications. Additionally, undesirable secondary products including dialkyl or glycerol ethers due to etherification reactions under higher temperature can also be obtained in the solid acid-catalyzed reaction systems.[38]

Goodwin Jr. and co-workers have revealed the reasons of lower catalytic activity of acid-catalyzed transesterification reaction with respect to base-catalyzed transesterification reaction through studying the mechanism of acid- and base-catalyzed transesterification reaction. For the acid-catalyzed transesterification reaction, the protonation of carbonyl group on TG molecule by Brønsted acid is the key step in the catalyst–TG interaction. However, this initial chemical pathway in turn increases the electrophilicity of the adjoining carbon atom, resulting in the intermediate molecules susceptible to nucleophilic attack of alcohol. In the last step, the intermediate is broken down to FAME accompanying with the release of proton. In contrast, the base catalysis takes on a more direct route, at which alkoxide ion (RO^-), the active species that is responsible for converting TG to FAME, is created initially and directly acts as a strong nucleophile to attack carbonyl group, accordingly, a tetrahedral intermediate can be formed. This crucial different pathway (formation of electrophilic species by acid catalysis *vs* formation of stronger nucleophile by base catalysis) is ultimately responsible for the difference in catalytic activity in transesterification reaction between acid and base catalyst.[15]

Thereby, careful design of robust, efficient and stable solid acid catalysts that can improve the efficiency of biodiesel production dramatically is still an important challenge. The ideal solid acid catalyst for esterification and transesterification reactions should have characteristics such as strong Brønsted and/or Lewis acid properties, unique porosity or textural properties and a hydrophobic surface. On the other hand, deactivation, poisoning and leaching of acid sites in the reaction medium should be avoided. Having these points in mind, the next sections will summarize the recent advances in the biodiesel production by novel solid acid catalysts. A particular focus of this perspective will be design of organic-inorganic hybrid acid catalysts for biodiesel production under mild conditions (*i.e.* refluxing temperature of alcohol and atmospheric pressure). Additionally, the influence of the acidity, porosity as well as surface hydrophobicity on the acid catalytic activity and stability of as-prepared multifunctionalized hybrid catalysts will be revealed.

3. Design of solid acid catalysts for biodiesel production

3.1 Influence of solid acid strength

The Brønsted acid sites are highly polarized hydroxyl groups at the surface of the catalyst that serve as the H^+-donor, while the Lewis acid sites are coordinatively unsaturated cationic sites, which leave the exposed M^+ ion to interact with guest molecules and act as the acceptor of the electron-pair.[39] The ideal solid acid catalyst for biodiesel production would be bifunctional, containing both Brønsted and Lewis acid sites with a hydrophobic environment protecting the Lewis site from the poisoning effect of water. Both Brønsted and Lewis acid sites can promote the esterification and transesterification reactions; moreover, Lewis acid sites are more active in promoting

transesterification reactions provided that the sites are not poisoned by water.[40] Since the lower catalytic activity of solid acids compared with solid bases, most of the solid acid-catalyzed esterification or transesterification reactions generally perform under higher temperature and higher pressure. Biodiesel production from typical solid acid catalysts is summarized below.

3.1.1 Sulfated metal oxides

Sulfated metal oxides such as SO_4^{2-}/ZrO_2, SO_4^{2-}/Ta_2O_5, SO_4^{2-}/Nb_2O_5 and SO_4^{2-}/TiO_2 are typical solid superacids, and they possess potential economic and green benefits for a wide variety of hydrocarbon reactions under mild conditions and are of interest for esterification and transesterification.[41–44] ZrO_2 (or Ta_2O_5, Nb_2O_5, TiO_2) itself possesses both Brønsted and Lewis acid acidity that can protonate pyridine and coordinatively bound to pyridine simultaneously.[35,45] The Brønsted acidity of ZrO_2 (or Ta_2O_5, Nb_2O_5, TiO_2) can be further enhanced by modifying its surface with sulphate group.[46] As shown in Fig. 3, in one SO_4^{2-}/ZrO_2 unit, two oxygen atoms from S–O bonds are bonded to Zr atoms in addition to coordination of a S=O group with a Zr atom, and the acidic proton is derived from the surface hydroxyl group of ZrO_2 induced by sulphate group. This acidic proton can be released easily owing to three S–O–Zr bonds link one SO_4^{2-} group with the ZrO_2 matrix, resulting in the strong Brønsted acidic strength of the SO_4^{2-}/ZrO_2. The above explanation is also suitable for SO_4^{2-}/Ta_2O_5, SO_4^{2-}/Nb_2O_5 and SO_4^{2-}/TiO_2; moreover, the Brønsted acid strength of sulfated metal oxide is significantly influenced by electronegativity of the metal element. Generally, lower electronegativity of the metal element, weaker M–OH (M = Zr, Ta, Nb or Ti) bond is expected; accordingly, the release of the protons is more easily. The electronegativity order of the corresponding metal is Zr (1.33) < Ta (1.50) < Ti (1.54) < Nb (1.60), which is consistent with the Brønsted acid strength order of the materials, *i.e.* $SO_4^{2-}/ZrO_2 > SO_4^{2-}/Ta_2O_5 > SO_4^{2-}/Nb_2O_5 > SO_4^{2-}/TiO_2$).[47]

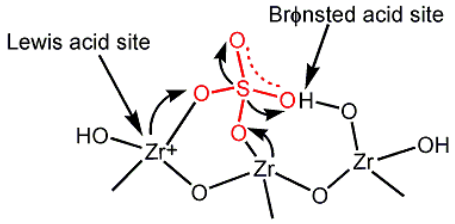

Fig. 3 Illustration of the Brønsted and Lewis acid sites in SO_4^{2-}/ZrO_2 acid.

Since the highest Brønsted acid strength of SO_4^{2-}/ZrO_2 among various sulfated metal oxides, it is the most common solid acid used for biodiesel synthesis. Moreover, the Lewis acid sites of SO_4^{2-}/ZrO_2 can also catalyze FFA esterification and TG transesterification by direct coordination of FFA or TG to unsaturated surface Zr^{4+} sites.[48] For example, Rothenberg and co-workers found that SO_4^{2-}/ZrO_2 showed high catalytic activity and selectivity for the esterification of dodecanoic acid with 2-ethylhexanol, propanol and methanol at 120–180 °C. The initial rate of the SO_4^{2-}/ZrO_2 catalyzed esterification reaction was about three times higher compared to that of the catalyst-free reaction. After five consecutive runs, the activity dropped to 90% of the original value and remained constant thereafter. Re-calcination of this deactivated catalyst can restore it to the original activity.[16] However, Goodwin Jr. and co-workers found that significant activity loss of SO_4^{2-}/ZrO_2 occurred during recycling tests on transesterification of tricaprylin with methanol, ethanol and *n*-butanol at 120 °C and 6.8 atm.[49] The same conclusion was also drawn by other groups for the use of SO_4^{2-}/ZrO_2 in esterification and transesterification reactions.[50,51] Reason for SO_4^{2-}/ZrO_2 deactivation is due to a combination of sulphate group leaching, the blocking of the active sites by reactants and/or products and deposition.[52,53] Conventional preparation of SO_4^{2-}/ZrO_2 is *via* post-synthesis grafting method followed by calcination at relative high temperature (600–650 °C).[16] This route leads to relatively weak interactions between SO_4^{2-} ion and ZrO_2 framework and thereby poor catalytic stability of the SO_4^{2-}/ZrO_2; additionally, the prepared SO_4^{2-}/ZrO_2 possesses poor porosity such as small BET surface area and low pore volume, which limit its inherent catalytic activity. By designing new preparation routes and changing the preparation conditions, the porosity of SO_4^{2-}/ZrO_2-based catalysts is expected to be improved; meanwhile, interaction between SO_4^{2-} ion and ZrO_2 framework is expected to be strengthened. Accordingly, the enhanced catalytic activity and stability can be obtained, leading to SO_4^{2-}/ZrO_2-based catalysts more extensive applications in biodiesel production under mild conditions. For example, Srinophakun's group recently reported that SO_4^{2-}/ZrO_2 prepared by a solvent-free method exhibited high catalytic activity in esterification of myristic acid with methanol in presence of TGs under the conditions of 120 to 150 °C, catalyst loading of 1 to 3 wt.% and methanol-to-oil molar ratio of 1: 4 to 1: 20. Reusability evaluation showed that deactivation of as-prepared SO_4^{2-}/ZrO_2 is *ca.* 10% after five consecutive runs, originating from leaching of sulfate groups into the reaction media.[44] Jiménez-López's group reported a series of new SO_4^{2-}/ZrO_2-based catalysts obtained by calcined zirconium sulfate supported on MCM-41 silica (Zr*X*-MCM, where *X* is the weight percentage of zirconium sulfate precursor) for ethanolysis of sunflower oil with high FFA and water contents. Under the conditions of ethanol-to-sunflower oil molar ratio of 12: 1, 5 wt.% of catalyst loading, 200 °C and 6 h, Zr30-MCM catalyst exhibited the highest yield of ethyl esters of fatty acids (91.5 %). Moreover, as-prepared catalysts are stable and maintain similar catalytic activity after three catalytic cycles, accompanying with no leaching of sulfate species into the reaction medium.[54]

3.1.2 Sulfonic ion-exchange resin

The representatives of the main classes of sulfonic ion-exchange resins including Amberlyst resins (*e.g.* Amberlyst-15, -16, -35, -36 and -131),[55,56] Nafion resins (*e.g.* Nafion SAC-13 and NR50)[57–61] and EBD resins (*e.g.* EBD-100, -200 and -300)[62] are the most common heterogeneous acid catalysts used and have proven to be effective in liquid phase esterification and transesterification reactions (Table 1). These strong acidic ion-exchange resins have a cross-linked polymeric matrix on which the active sites for the esterification and transesterification reactions are the protons bonded to sulfonic groups.[63] Additionally, the catalytic activity of the resins depends strongly on their swelling properties since swelling capacity dominates surface area and pore diameter of resins, which in turn influence the population of acid sites and accessibility of the reactants to the acid sites and hence their overall reactivity.[7] The relatively high sulfonic acid loadings on polystyrene sulfonic acid resins (with respect to sulfonic acid catalysts on inorganic supports) combined with their ready availability makes these materials

Table 1 Recent typical examples on the use of sulfonic ion-exchange resins in biodiesel production[a]

Catalyst	Biodiesel production				Ref
	Feedstocks	Reaction conditions	Activity	Recyclability	
Amberlyst-15	Dodecanoic acid 2-ethylhexanol (esterification)	2-ethylhexanol-to-dodecanoic acid molar ratio = 1: 1; 2 h; 150 ^{o}C; Catalyst amount 3 wt.%	Conv. (%) = 98	Deactivation after 2 h	[16]
Amberlyst-15 Amberlyst-16 Amberlyst-131	Oleic acid/soybean oil at 50% of acidity (Esterification)	Methanol-to-oleic acid molar ratio = 8: 1; 100 ^{o}C, 5 h; Catalyst amount 2.5 wt.%	Conv. (%) = 85 Conv. (%) = 88 Conv. (%) = 90	Not studied	[63]
Nafion SAC-13 (Nafion/SiO_2)	Acetic acid Propionic acid Butyric acid Hexanoic acid Caprylic acid (Esterification)	Methanol-to-acid molar ratio = 2: 1; 60 ^{o}C; Catalyst amount 2.5 wt.%	TOF (HAc, min^{-1}) = 7.3 TOF (HPr, min^{-1}) = 4.8 TOF (HBu, min^{-1}) = 2.9 TOF (HHx, min^{-1}) = 2.2 TOF (HCp, min^{-1}) = 1.5	Without any treatment of the used catalyst: significant deactivation after three cycles; THF washing is able to improve catalyst reusability	[57,58]
Purolite D5081 and D5082	Oleic acid (Esterification)	Methanol-to-oleic acid molar ratio = 44: 1; 65 ^{o}C; Catalyst amount 5 wt.% (referred to acid)	TOF (D5081, h^{-1}) = 65.0 TOF (D5082, h^{-1}) = 26.0	Catalytic activity is substantially lost after the first run; the activity remains stable on repeated uses if the reaction was carried out at 85 ^{o}C	[64]
EBD-100 EBD-200 EBD-300	Synthetic mixture of stearic acid and sunflower or rapeseed oil; Old frying oil (Preesterification of FFAs)	Methanol-to-FFA molar ratio = 19.7: 1 (synthetic mixture) and 12.2: 1 (old frying oil); 65 ^{o}C; 24 h; Catalyst amount 1.0 wt.%	Conv. (%) = 100 Conv. (%) = 100 Conv. (%) = 81	Fast catalyst deactivation caused by continuous ion-exchange with trace salt contaminants	[62]

[a] All resin catalysts presented are commercial available.

particularly attractive as esterification or transesterification catalysts.[64]

Amberlyst-15 is one of the macroporous polystyrene/divinylbenzene resin-based sulfonic ion-exchange resins that are commonly used in biodiesel production. For example, Amberlyst-15 (BET surface area 50 m^2 g^{-1}) used in esterification of dodecanoic acid with 2-ethylhexanol at 150 ^oC showed high catalytic activity at the early stage of the reaction but deactivated after 2 h.[16] Nafion resins (*e.g.* Nafion NR50) are sulfonic acid supported on fluorinated polymers, while Nafion SAC-13 (BET surface area 196 m^2 g^{-1}) is a composite material, combining Nafion and a porous silica (Nafion/SiO_2). The latter is known to exhibit relatively strong acid property. Both of the resin catalysts showed excellent catalytic activity in transesterification and esterification reactions and tended to maintain higher catalytic activities, especially when water byproduct was stripped off during the reaction. For example, esterification of various carboxylic acids including acetic, propionic, butyric, hexanoic and caprylic acid with methanol at 60 ^oC catalyzed by Nafion SAC-13 was investigated by Goodwin Jr.'s group, and the impact of carboxylic acid chain length on the catalytic activity of SAC-13 was revealed. It was found that reaction rate decreased as the number of carbons in the linear alkyl chain increased, which is explained in terms of the polar and steric effects of the alpha-substituent to the carboxylic group. The research also concluded that the important parameters, such as water deactivation and catalyst reusability and regeneration, were also affected by the size of the carboxylic acids used. Using THF washing, the Nafion/SiO_2 nanocomposite catalyst showed good reusability in esterification of shorter chain carboxylic acids like butyric acid, but the catalyst experienced continuous activity loss in consecutive reaction cycles using longer chain carboxylic acids like HCp. They explained that the catalyst deactivation was probably due to accumulation of the carboxylic acid molecules/intermediates on/in the nanodomains of the Nafion resin. Such an accumulation may have been caused by the irreversible adsorption of carboxylic acids on Brønsted sites and/or their entanglement with the polymeric chains of the Nafion nanoparticles. Accordingly, effective regeneration is needed to improve the applicability of SAC-13 in the esterification of large FFAs.[57,58]

EBD resins are new sulfonic acid functionalized polystyrene/divinylbenzene copolymers, and they are classified into two main types, *i.e*, microporous gelular (*e.g*. EBD-100, Fig. 4a) and macroporous resins (*e.g*. EBD-200 and -300, Fig. 4b and c). Gelular EBD resins have a low cross-linking degree of 5–8% divinylbenzene and small micropores (1 nm in pore diameter), while macroporous EBD resins have a high cross-linking degree of 12–20% divinylbenzene and macropores (100 nm in diameter). Russbueldt and Hoelderich have investigated the preesterification of various FFA-containing oils with methanol by aforementioned three EBD resins.[62] They found that the catalytic performance of the gelular sulfonic resin EBD-100 was superior to the macroporous catalysts EBD-200 and -300. This result is possibly explained by the more dense gel matrix and poor methanol uptake of the macroporous EBD-200 and -300, while the low crosslinked gelular EBD-100 is swelling in methanol to a greater extent. Additionally, the acid sites in the resin matrix of the gelular material are accessible for the esterification, while the reaction takes only place on the superficial sulfonic acid groups for the macroporous resins. A major challenge of application of EBD resins in FFA esterification reactions is the fast catalyst deactivation caused by continuous ion-exchange with trace salt contaminants (*e.g*. Na^+, K^+, Mg^{2+} and Ca^{2+}) of the oily feedstocks, however, the deactivation is a completely reversible effect, and regeneration with hydrochloric acid washing can restore the original activity.

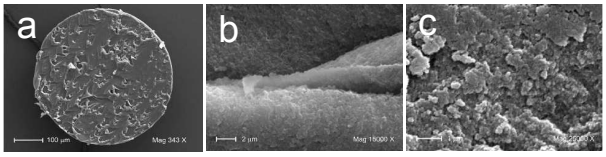

Fig. 4 SEM images of (a) EBD-100; (b) EBD-200 and (c) EBD-300. (Adapted from ref. 62 with permission from ELSEVIER)

More recently, new acid resins, sulphonated hypercrosslinked polystyrene resins such as Purolite D5081 (BET surface area 701 m^2 g^{-1}) and D5082 (BET surface area 381 m^2 g^{-1}), have been successfully applied in the esterification of oleic acid with methanol at 65 ^oC. At the same catalyst amount, conversion of oleic acid was the highest for D5081 (or D5082) among all tested sulfonic ion-exchange resins including Amberlyst-15, Amberlyst-35 and Nafion SAC-13 although the hypercrosslinked resins exhibited relatively low concentrations and strengths of acid sites compared with the tested conventional polystyrene/divinylbenzene sulphonic acid resins. Brown and co-workers concluded that the excellent accessibility for reactant molecules to sulfonic acid groups of hydrophobic hypercrosslinked resins is responsible for this unique esterification reactivity. However, the esterification activity of D5081 resin is significantly and irreversibly reduced after just one use when the reaction temperature is 65 ^oC, but activity is maintained when the higher reaction temperature of 85 ^oC is used. It is speculated that the activity loss is related to the blockage and deposition of the fine pores in the hypercrosslinked resin by large fatty acid molecules at lower temperature. At higher temperature, it is suggested that pore blockage and deposition hardly occurs because of fast diffusion of fatty acid molecules, and therefore, the activity of D5081 is retained for multiple cycles without the need for catalyst regeneration.[64]

Sulfonic ion-exchange resins also exhibited considerably high catalytic activity towards biodiesel produced from simultaneous esterification and transesterification of low-cost feedstocks in packed column reactor. For example, under the optimal conditions, biodiesel production from waste cooking oil, soybean oil deodorizer distillate, rapeseed oil deodorizer distillate and stale inedible oil catalyzed by resin D002 afforded FAMEs yields in the range from 85.5 to 97.1% (Table 1). Moreover, it also manifested very excellent operational stability after repeated uses. Therefore, compared with biodiesel production carried out in a batch reactor, biodiesel synthesis from waste oil in a packed column reactor has application potentials.[65]

3.1.3 Sulfonic acid modified mesoporous silica

Templated mesoporous silica materials, *e.g*. SBA and MCM series of inorganic silica and periodic mesoporous organosilica (PMO), possess abundant surface silanol groups as well as

Table 2 Recent typical examples on the use of sulfonic acid modified mesoporous (organo)silica in biodiesel production

Catalyst	Biodiesel production					Ref
	Preparation method	Feedstocks	Reaction conditions	Activity	Recyclability	
Propyl-SO_3H SBA-15 Arene-SO_3H SBA-15 Me/Arene-SO_3H SBA-15	Co-condensation Co-condensation Post-synthesis	Soybean oil containing 20 wt.% of oleic acid (esterification and transesterification)	Microwave irradiation; 1-butanol-to-oil molar ratio = 6: 1 190 °C; 15 min; Catalyst amount 5 wt.%	Yield (%) = 38 Yield (%) = 56 Yield (%) = 58	The activity level of the 2nd run was 85–90% of the fresh catalyst activity	[66]
Propyl-SO_3H-KIT-6 (5.2 nm) Propyl-SO_3H-KIT-6 (6.2 nm) Propyl-SO_3H-KIT-6 (7.0 nm)	Post-synthesis	Palmitic acid (esterification)	Methanol-to-palmitic acid molar ratio = 30: 1; 60 °C; atmospheric pressure; 6 h Catalyst amount 0.4 wt.%	Conv. (%) = 14 Conv. (%) = 28 Conv. (%) = 39	Stable under the mild operating conditions employed	[67]
SBA-15-SO_3H SBA-15-SO_3H-R R/SBA-15-SO_3H (R = Me, Et or Ph)	Co-condensation Co-condensation Post-synthesis	Palmitic acid in soybean oil (esterification)	Methanol-to-palmitic acid molar ratio = 20: 1; 85 °C; 2 h; Catalyst amount 10 wt.%	Conv. (%) = 88 Conv. (%) = 84 Conv. (%) = 70	No data about deactivation behaviour	[68]
PrSO_3H-MM-SBA-15	Post-synthesis	Palmitic acid Glyceryl trioctanoate (esterification and transesterification)	Methanol-to-palmitic acid molar ratio = 4: 1; Methanol-to-glyceryl trioctanoate molar ratio = 30: 1; 60 °C; 6 h; Catalyst amount 0.3 wt.%	Conv. (%) of palmitic acid = 55; Conv. (%) of glyceryl trioctanoate = 2.5	No data about deactivation behaviour	[69]

tunable porosity and morphology, which ensure them being easily functionalized by sulfonic acid groups; meanwhile, the resulting sulfonic acid modified mesoporous silica generally possess large surface area, uniform pore-size distribution, high pore volume and tunable dimensionality of the pore channels and structural orderings.

Sulfonic acid functionalized silica materials prepared by using tetraethoxysilane as silica precursor are widely applied to catalyze esterification and transesterification reactions (Table 2). For instance, Lane's group has prepared a series of organosulfonic acid functionalized SBA-15 catalysts such as propyl-SO_3H SBA-15 and arene-SO_3H SBA-15 by one-step co-condensation route, and the catalysts exhibited high activity in the microwave-assisted simultaneous transesterification and esterification of soybean oil containing 20 wt.% of oleic acid with 1-butanol; moreover, at the same functional group loading and experimental conditions, arene-SO_3H SBA-15 showed higher transesterification activity than that of propyl-SO_3H SBA-15. The authors explained that this activity difference mainly depended on the acid strength instead of the number of acid sites as well as textural properties (both of the catalysts possessed comparable acid capacity and textural properties). The different nature of the molecular environment of the $-SO_3H$ sites in propyl-SO_3H SBA-15 and arene-SO_3H SBA-15 catalysts defined their acid strength. For arene group, it can provide stronger electron withdrawing environments than propyl group, leading to arene-SO_3H SBA-15 higher Brønsted acid strength and thereby higher catalytic activity in both target reactions than that of propyl-SO_3H SBA-15. Due to the highly hydrophobic nature of both soybean oil and FAMEs, their molecular transport within the pore framework is expected to be especially affected by surface interactions. Meanwhile, sulfonic acid functionalized silica catalysts often suffer from severe deactivation due to accumulation of organic or carbonaceous materials on the surface that blocks the acidic sites; additionally, leaching of sulfonic acid group into the reaction media may also reduce the catalytic activity after several times' reaction cycles. Therefore, arene-SO_3H SBA-15 catalyst was further functionalized with methyl silyl groups to increase its surface hydrophobicity with an attempt to improve its catalytic performance. It was found that methyl-functionalized arene-SO_3H SBA-15 catalyst was only slightly more active than the unmodified arene-SO_3H SBA-15 catalyst; meanwhile, reuse of this catalyst after solvent washing gave a similar activity recovery as arene-SO_3H SBA-15.[66] The influence of the incorporated alkyl group on the catalytic performance of the sulfonic acid modified mesoporous silica catalysts should be studied further, and it is expected that significant enhanced catalytic activity and stability of the hydrophobic group modified SO_3H-SBA-15 catalysts may be obtained by designing suitable preparation routes and selecting the optimum alkyl group loading.

Other new inorganic silica support like KIT-6 with tunable pore diameter (5.2, 6.2 or 7.0 nm) were also used to prepare sulfonic acid modified mesoporous silica catalysts, which has been reported by Wilson's group. KIT-6 propylsulfonic acid silicas with *Ia3d* pore architecture ($PrSO_3H$-KIT-6) and different pore diameters were prepared by a post grafting procedure, and they were applied in the esterification of shorter (*e.g* propanoic and hexanoic acid) and longer chain FFAs (*e.g*. lauric and palmitic acids) with methanol under atmospheric pressure and refluxing conditions. It was found that the interconnected pore network as well as enlarged pore diameter of KIT-6 over SBA-15 (two-dimensional ordered pores with pore diameter of 4.9 nm) can improve mass transport and pore accessibility, leading to $PrSO_3H$-KIT-6 enhanced esterification activity compared with $PrSO_3H$-SBA-15 (Fig. 5).[67]

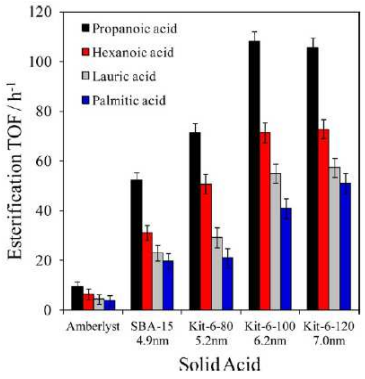

Fig. 5 Comparative performance of $PrSO_3H$-SBA-15 and $PrSO_3H$KIT-6 series versus Amberlyst 15 in propanoic, hexanoic, lauric, and palmitic acid esterification with methanol at 60 °C. (Adapted from ref. 67 with permission from ACS.)

In addition to the flexibility in pore diameter, the performance of organosulfonic acid-functionalized mesoporous silica can be improved further by the selective exclusion of unwanted molecules that can inhibit the reactants from approaching $-SO_3H$ sites (*e.g*. hydrophilic products water and glycerol in esterification of FFAs and transesterification of TGs). The motivation was realized by incorporation of hydrophobic organic groups (*e.g*. methyl, ethyl and phenyl) into organosulfonic acid-functionalized mesoporous silica materials by postsynthesis grafting and one-step co-condensation methods.[68] The research results from the reaction of esterification of palmitic acid in soybean oil with methanol indicated that the overall conversion of the co-condensed catalysts (SBA-15-SO_3H-R, R = Me, Et or Ph) is similar to that of the unmodified SBA-15-SO_3H, however, the grafted catalysts (R/SBA-15-SO_3H, R = Me, Et or Ph) actually led to a decrease in catalyst performance relative to the reference catalyst SBA-15-SO_3H; additionally, the co-condensed catalysts gave higher initial catalytic activity than that of SBA-15-SO_3H. The studies also indicated that no significant difference between the catalytic performances of the different alkyl groups on the multifunctionalized mesoporous silica materials was observed, despite the differences in their degree of hydrophobicity. Therefore, it is concluded that both hydrophobicity and textural properties of multifunctionalized mesoporous silica materials influence the catalytic activity of the hybrid catalysts in the esterification of palmitic acid.

In order to accommodate bulky and viscous C_{16}–C_{18} TG molecules and alleviate their diffusional problems in the transesterification process, propylsulfonic acid functionalized, hierarchical macroporous–mesoporous SBA-15 silica catalysts have been successfully synthesised *via* dual-templating routes employing liquid crystalline surfactants and polystyrene beads followed by post-functionalization of propylsulfonic acid groups (Fig. 6). The prepared bi-modal $PrSO_3H$-MM-SBA-15 catalysts

offered high surface areas and well-defined, interconnecting macro- and mesopore networks with respective narrow size distributions around 300 nm and 3–5 nm. The incorporation of such macropores is found to confer a striking enhancement in both the rate of transesterification of tricaprylin and esterification of palmitic acid with methanol under 60 °C, which is attributed to the greater accessibility of $-SO_3H$ sites within the mesopores due to macropores acting as rapid transport conduits to the active sites and enhancing mass-transport. The studies pave the way to the wider application of hierarchical catalysts in biofuel synthesis and biomass conversion.[69,70] However, from viewpoint of practical applications the recyclability of the materials should be evaluated.

More recently, sulfonic acid modified alkyl-bridged PMO materials have been developed, and they were applied in some acid-catalyzed reactions including dehydration of monosaccharides and polysaccharides to 5-hydroxymethylfurfural.[71] PMOs, prepared by condensation of bissilylated organic precursors, $(R'O)_3Si{-}R{-}Si(OR')_3$ (*e.g.* R = $-C_2H_4-/-C_6H_4-/-C_6H_4-C_6H_4-$; R' = $-CH_3/-C_2H_5$), have higher hydrothermal stabilities compared with mesoporous inorganic silica with purely inorganic frameworks, presumably because of their lower water affinity. Hydrophobicity and other chemical properties can be tuned by varying the organic groups present in the hybrid organic-inorganic framework.[72] It is expected PMO-based sulfonic acid catalysts may also be the promising catalysts in biodiesel production.

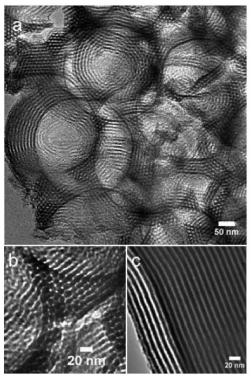

Fig. 6 HRTEM of: a) hierarchical macro and mesopore structures in MM-SBA15-4; b) high resolution image of hexagonal mesoporous arrays in MM-SBA15-4 and c) mesoporous channels in MM-SBA15-2. (Adapted from ref. 69)

3.1.4 Sulfonated carbon-based catalyst

Sulfonated carbon-based catalysts can be readily prepared by incomplete carbonization of sulfopolycyclic aromatic compounds in conc. H_2SO_4[73] or sulfonation of incompletely carbonized natural organic matter such as D-glucose, sucrose, cellulose and starch.[37,74–77] These catalysts are highly effective and can be recycled towards the conversion of low-cost feedstocks containing higher FFAs to biodiesel (Table 3).

More recently, cellulose-derived carbon solid acids (CCSAs) have been widely applied in biomass conversion-related reactions, such as esterification, transesterification, hydrolysis and dehydration. Among them, SO_3H-bearing CCSA materials have attracted particular attentions.[78] The materials can incorporate large amounts of hydrophilic molecules, including water, into the carbon bulk, due to the high densities of hydrophilic functional groups (*e.g.* –COOH, –OH and $-SO_3H$) bonded to the flexible carbon sheets (Fig. 7). Such incorporation provides good access by reactants in solution to the SO_3H groups, which gives rise to high catalytic performance despite the small surface area of the materials (< 2 m^2 g^{-1}). For example, Hara's group prepared a carbon material functionalized with $-SO_3H$ groups by using microcrystalline cellulose powder as the starting material and fuming sulfuric acid as the $-SO_3H$ source. This material is amorphous carbon consisting of $-SO_3H$, –COOH and phenolic OH-bearing nanographene sheets in a considerably random manner. As-prepared sulfonated carbon-based material exhibited much higher catalytic activity for the esterification of oleic acid with methanol than other conventional solid Brønsted acid catalysts including niobic acid or sulfonated polystyrene-based cation-exchangeable resins, and it is *ca*. 60% as active as H_2SO_4 under the same reaction conditions. The strong acidity of the catalyst is due to the fact that some of the $-SO_3H$ groups in the carbon materials are linked by strong hydrogen bonds, which can result in strong acidity due to mutual electron-withdrawal.[76,79,80] After washing with water and drying at 130 °C, the used SO_3H-bearing CCSA catalyst can be reused 10 times without decrease in activity. Therefore, the CCSA material can function as an efficient and reusable catalyst for the conversion of FFAs to FAMEs in low-cost oily feedstocks. The carbon material also showed high catalytic performance for transesterification of triolein proceeded at 130 °C and 700 kPa, and its activity outperformed conventional solid acids such as silica-supported Nafion (Nafion SAC-13), Amberlyst-15 and Nafion NR50. Over period of 6 h, the yield of methyl oleate reached 24.1 (SO_3H-bearing CCSA), 5.0 (Amberlyst-15), 1.5 (Nafion NR50) and 1.1% (Nafion SAC-13). After washing with water and drying at 130 °C, the used SO_3H-bearing CCSA catalyst can be reused 5 times without decrease in activity.

Zong and Smith have reported that sulfonated D-glucose-derived sugar catalyst showed higher catalytic activity towards esterification of palmitic acid, oleic acid and stearic acid with methanol compared with niobic acid, Amberlyst-15 and sulfated zirconia. Moreover, it had excellent operational stability, and after more than fifty cycles of successive re-use, it still retained a remarkably high proportion (93%) of its original catalytic activity in the methyl oleate formation reaction. Therefore, this sugar catalyst is very promising to replace H_2SO_4 as a green catalyst for efficient production of biodiesel from higher fatty acids and especially waste oils with a high acid value.[74] Fuertes's group reported that the sulfonated carbon microspheres, prepared by sulfonation of hydrothermal carbonized glucose-derived carbonaceous microspheres, exhibited remarkably high catalytic activity towards the esterification of oleic acid with ethanol at 55 °C. Under the same conditions, its catalytic activity is superior to Amberlyst-15.[81] More recently, Dong and co-workers prepared a multifunctionalized ordered mesoporous carbon (OMC)-based solid catalyst ($OMC{-}H_2O_2{-}SO_3H$) *via* a simple oxidation treatment of OMC followed by sulfonation. This $-SO_3H$ group functionalized carbon material possesses both hydrophilic groups ($-SO_3H$, –COOH, –OH) and the hydrophobic framework (polycyclic aromatic carbon) as well as high density of $-SO_3H$ groups, large surface area, high pore volume and narrow pore size

distribution, which lead to it evidently improved catalytic activity

Table 3 Recent typical examples on the use of sulfonated carbon-based catalyst in biodiesel production

Catalyst	Biodiesel production					Ref
	Preparation method	Feedstocks	Reaction conditions	Activity	Recyclability	
SO_3H-bearing CCSA	Sulfonation of incompletely carbonized microcrystalline cellulose powder	Oleic acid Triolein (esterification and transesterification)	Methanol-to-oleic acid molar ratio = 26: 1; 95 °C; 4 h; Catalyst amount 4 wt.% (esterification); Methanol-to-triolein molar ratio = 62: 1; 130 °C; 700 kPa; 5 h; Catalyst amount 7.3 wt.% (transesterification)	Esterification yield (%) = 100 Transesterification Yield (%) = 98	Esterification and transesterification can be reused 10 and 5 times without decrease in activity	[78]
Sulfonated D-glucose-derived sugar catalyst	Sulfonation of incompletely carbonized D-glucose	Palmitic acid Oleic acid Stearic acid (esterification)	Methanol-to-acid molar ratio = 10: 1; 65 °C; 5 h; Catalyst amount 5 wt.% (related to acid)	Yield (%) > 95	Stable after fifty cycles of successive re-use	[74]
OMC−H_2O_2−SO_3H	Sulfonation of H_2O_2-treated OMC	Palmitic acid Oleic acid Stearic acid (esterification)	Methanol-to-oleic acid molar ratio = 20: 1; 80 °C; 2 h	Conv. (%) = 80	No obvious activity loss after 5 successive cycles	[82]
Sulfonated vegetable oil asphalt- and petroleum asphalt-derived solid acids	Sulfonation of an incompletely carbonized vegetable oil asphalt and petroleum asphalt	Waste oil containing 50 wt.% of oleic acid and 50 wt.% of cottonseed oil (esterification and transesterification)	Methanol-to-waste oil molar ratio = 20.9: 1; Catalysts amount 0.3 wt.% (related to waste oil)	Waste oil conv. (%) = 95 (only having the reaction proceeded at 220 °C; 5 h); Waste oil conv. (%) = 98 (coupling reaction and separation; 3 h; 140 and 220 °C for the first and second step)	Recoverable	[84]

for the synthesis of FAMEs from esterification of aliphatic acids like oleic acid, palmitic acid and stearic acid with methanol or ethanol. Furthermore, the catalyst can retain its initial activity after at least five consecutive catalytic cycles.[82]

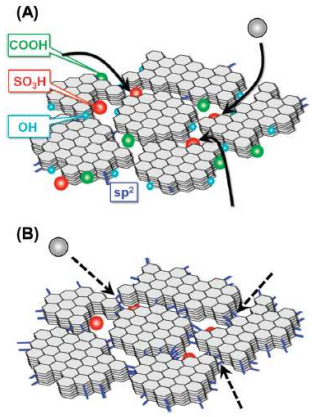

Fig. 7 Schematic structures of proposed SO_3H-bearing CCSA materials carbonized at different temperatures: (a) CCSA carbonized below 723 K and (b) CCSA carbonized above 823 K. (Adapted from ref. 78 with permission from ACS.)

To date, studies on the biodiesel production from transesterification of TG-containing feedstocks catalyzed by sulfonated carbon-based catalysts are few. Wang's group recently developed a carbon-based solid acid catalyst by sulfonation of carbonized vegetable oil asphalt and petroleum asphalt, and the catalyst consisted of a flexible carbon-based framework with highly dispersed polycyclic aromatic hydrocarbons containing sulfonic acid groups. This carbon-based solid acid exhibited high catalytic activity for simultaneous esterification and transesterification of a waste vegetable oil containing large amounts of FFAs, and the maximum conversion of TG and FFA reached 80.5 and 94.8% under the conditions of 4.5 h, 220 °C, methanol-to-oil molar ratio of 16.8: 1 and catalyst/mixed oil mass ratio of 0.2 wt.%. They explained that the high catalytic activity is ascribed to the high acid site density, the hydrophobicity of its carbon sheet that prevented the hydration of –OH group as well as the bonded $-SO_3H$ hydrophilic functional groups that allowed more methanol to contact the protonated carboxylic group of FFA or TG.[83,84] Design of more efficient and stable carbon-based solid acid catalysts for transesterification of TGs under mild conditions is still a challenge.

3.1.5 HPAs and supported HPAs

HPAs are a type of solid acid that is composed of early transition metal (V, Nb, Mo, Ta or W)-oxygen anion clusters with unique and well-defined structure, and they are regarded as environmentally benign and economically feasible alternatives to conventional acid catalysts due to their super strong Brønsted acidity, high proton mobility, nontoxicity and stability.[85–88] In the field of acid catalysis, the most common and widely used HPAs are Keggin-type $H_3PW_{12}O_{40}$ and Wells–Dawson-type $H_6P_2W_{18}O_{62}$, and they have exhibited excellent catalytic behaviors in a wide variety of acid-catalyzed reactions including alkylation and acylation of hydrocarbons, hydration of alkenes and polymerization of THF.[89–91] Recent research has found that HPAs also can be used as catalytic systems for biomass conversion to biofuel or other value-added important organic intermediates (Table 4).[3] For instances, Keggin-type HPAs including $H_3PW_{12}O_{40}$, $H_4SiW_{12}O_{40}$, $H_3PMo_{12}O_{40}$ and $H_4SiMo_{12}O_{40}$ have been applied in transesterification of rapeseed oil with methanol and ethanol, and they exhibited outstanding catalytic activity that was comparable to H_2SO_4 under the conditions of 85 °C and atmospheric pressure. This excellent transesterification activity is explained in term of higher acid strength of HPAs compared with that of H_2SO_4. Additionally, it is also observed that $H_3PMo_{12}O_{40}$ showed the highest TG conversion (55%) among all tested HPAs catalysts, owing to the fact that the crystallization water of $H_3PMo_{12}O_{40}$ is almost lost completely upon the thermal treatment at 120 °C and thereby the Brønsted sites solvation is suppressed.[92] Thereafter, Wang's group found that $H_3PW_{12}O_{40}$ was also effective for esterification of palmitic acid and transesterification of waste cooking oil. The yield of methyl palmitate reached 97% under the conditions of 65 °C, methanol-to-acid molar ratio of 2.5: 1, $H_3PW_{12}O_{40}$ loading 4 wt.% and 12 h. As for the transesterification of waste cooking oil, the highest yields of methyl esters (87%) was achieved under the conditions of 65 °C, methanol-to-oil molar ratio 70: 1, $H_3PW_{12}O_{40}$ loading 0.5 wt.% and 14 h.[93]

Nevertheless, HPAs show high solubility in polar media, and the above HPA-catalyzed esterification and transesterification reactions carried out in homogeneous rather than heterogeneous systems. As a consequence, it needs tedious procedures such as extraction or distillation to separate HPAs from the reaction media for the next catalytic cycle. Additionally, the specific surface area of bulk HPAs is extremely small (smaller than 5 $m^2 g^{-1}$), which limits their inherent catalytic activity due to the lack of number of available acid sites. To solve both of the problems, the following two effective strategies were developed. Firstly, partial or total substitution of protons in Keggin-type $H_3PW_{12}O_{40}$ with larger monovalent cations such as Cs^+, which leads to $Cs_xH_{3-x}PW_{12}O_{40}$ (x = 0.5–3.0) solid catalysts that are insoluble in polar solvents. Additionally, the specific surface area of $Cs_xH_{3-x}PW_{12}O_{40}$ increased significantly compared with bulk $H_3PW_{12}O_{40}$;[87] meanwhile, $Cs_xH_{3-x}PW_{12}O_{40}$ materials with suitable Cs content possess strong Brønsted acid strengths that are similar to the bulk $H_3PW_{12}O_{40}$. For example, the BET surface area of $Cs_{2.5}H_{0.5}PW_{12}O_{40}$ and $Cs_{3.0}PW_{12}O_{40}$ is 125.8 and 150.0 $m^2 g^{-1}$, respectively,[94] and the Brønsted acid strength of $Cs_xH_{3-x}PW_{12}O_{40}$ with x = 2.0–2.3 is $\triangle H_{ads}{}^0$ (NH_3) = – 150 KJ mol^{-1}.[91] $Cs_xH_{3-x}PW_{12}O_{40}$ catalysts have been successfully applied in simultaneous esterification of palmitic acid and transesterification of tributyrin with methanol under the conditions of acid/oil-to-methanol molar ratio of 1: 30 and 60 °C. For example, 100% palmitic acid conversion and 50.2% tributyrin conversion with 90% selectivity were achieved by using $Cs_{2.3}H_{0.7}PW_{12}O_{40}$ catalyst in only 6 h, and its catalytic activity outperformed SO_4^{2-}/ZrO_2, Nafion or H ZSM-5 under the same conditions. Furthermore, $Cs_{2.3}H_{0.7}PW_{12}O_{40}$ could be recycled at least three times without loss of activity and selectivity.[95]

The drawback of using Cs salts of HPAs is the formation of milky dispersion of the solid acids in the reaction media, which may lead to catalyst loss due to the difficulty in separation. As a result, the other strategy to fabricate water-tolerant HPAs by immobilization of HPA onto various inorganic or organic-inorganic porous materials (*e.g.* acidic metal oxides, acidic

Table 4 Recent typical examples on the use of HPAs and supported HPAs in biodiesel production

Catalyst	Biodiesel production					Ref
	Preparation method	Feedstocks	Reaction conditions	Activity	Recyclability	
$H_3PW_{12}O_{40}\cdot 24H_2O$ $H_3PMo_{12}O_{40}\cdot 28H_2O$ $H_4SiW_{12}O_{40}\cdot 24H_2O$ $H_4SiMo_{12}O_{40}\cdot 13H_2O$	Commercial available	Rapeseed oil (transesterification)	Ethanol-to-ester molar ratio= 6: 1; 60 °C and atmospheric pressure; 3 h; H^+ to ester molar percentage (%) 1.7–2.0	Conv. (mol%) = 27 Conv. (mol%) = 55 Conv. (mol%) = 20 Conv. (mol%) = 45	Not studied	[88]
$H_3PW_{12}O_{40}\cdot 6H_2O$	Commercial Available	Waste cooking oil (transesterification)	Methanol-to-oil molar ratio = 68: 1; Reactive distillation column combines with response surface methodology; Total feed flow = 116 mol h^{-1}; Feed temperature = 30 °C; Reboiler duty = 1.3 kW	Optium yield (%) = 94; Actual yield (%) = 94	Not studied	[150]
$C_{2.3}H_{0.7}PW_{12}O_{40}$	Ion exchange	Palmitic acid-containing tributyrin (simultaneous esterification and transesterification)	Methanol-to-oil/acid molar ratio = 30: 1; 60 °C; 6 h; Catalyst amount = 0.4 wt.%;	Conv. (%, palmitic acid) = 100; Conv. (%, tributyrin) = 50.2	Negligible activity loss after three cycles	[91]
$H_3PW_{12}O_{40}$/SBA-15	Post-synthesis	Oleic acid (esterification); Waste cooking oil (transesterification)	Methanol-to-oleic acid molar ratio = 40: 1; 40 °C; 4 h; Catalyst amount = 0.3 wt.%; $H_3PW_{12}O_{40}$ loading 23 wt.% (esterification) Methanol to oil volume ratio = 2: 1; 65 °C; 12 h (transesterification)	TOF (min^{-1}) = 9.3; (esterification) Conv. (%, waste cooking oil) = 75	No activity loss after four cycles	[107]
$H_3PW_{12}O_{40}$/Hβ	Post-synthesis	Oleic acid (esterification); Waste cooking oil and Jatropha oil (transesterification)	Methanol-to-oleic acid molar ratio = 20: 1; 60 °C; 6 h; Catalyst amount 1.1 wt.%; $H_3PW_{12}O_{40}$ loading 30 wt.% (esterification) Methanol-to-oil mass ratio = 8: 1; 60 °C; 20 h; Catalyst amount = 6 wt.% (referred to oil); (transesterification)	Conv. (%, oleic acid) = 84; Conv. (%, waste cooking oil) = 84; Conv. (%, Jatropha oil) = 93	No obvious decreased conversion of oleic acid after four cycles	[108]

Table 4 Continued

$H_3PW_{12}O_{40}/ZrO_2$ $H_3PW_{12}O_{40}/SiO_2$ $H_3PW_{12}O_{40}/Al_2O_3$ $H_3PW_{12}O_{40}/AC$	Post-synthesis	Canola oil containing 10% oleic acid (simultaneous esterification and transesterification)	Methanol-to-oil molar ratio = 6: 1; 200 °C; 600 psi; 10 h; Catalyst amount 3 wt.%; $H_3PW_{12}O_{40}$ loading 10 wt.%	Yield (%) = 77; Yield (%) = 65; Yield (%) = 65; Yield (%) = 65	No activity loss after recycling	[95]
$H_3PW_{12}O_{40}/Nb_2O_5$	Post-synthesis	Used cooking oil with 8% FFAs content	Methanol-to-oil molar ratio = 18: 1; 200 °C; 600 psi; 20 h; Catalyst amount 3 wt.%; $H_3PW_{12}O_{40}$ loading 25 wt.%	Yield (%) = 92	No considerable activity loss after five cycles	[97]
$H_3PW_{12}O_{40}/ZrO_2$	Post-synthesis	Oleic acid (esterification)	Methanol-to-oleic acid molar ratio = 6: 1; 100 °C, 4 h ; Catalyst amount 10 wt.%; $H_3PW_{12}O_{40}$ loading 20 wt.%	Conv. (%) of oleic acid = 88	80% of original activity was obtained after four cycles	[109]
Activated carbon fiber-supported HPAs ($H_3PW_{12}O_{40}$/ACF and $H_3PMo_{12}O_{40}$/ACF)	Post-synthesis	Palmitic acid (esterification)	Methanol-to-palmitic acid molar ratio = 97: 1; 60 °C; 6 h; Catalyst amount 1.4 wt.% ($H_3PMo_{12}O_{40}$/ACF), 1.1 wt.% ($H_3PW_{12}O_{40}$/ACF)	Conv. (%) = 76 ($H_3PMo_{12}O_{40}$/ACF) Conv. (%) = 88 ($H_3PW_{12}O_{40}$/ACF)	Obvious activity loss after the first cycle owing to HPA leaching	[106]

zeolites, silica, activated carbon and activated carbon fiber) has being emerged.[96–109] By using this method, the ease of HPAs separation for recycling use and increase their catalytic activity by improvement of the textural characters are realized simultaneously. For example, Dalai's group supported $H_3PW_{12}O_{40}$ on four solid supports including silica, alumina, hydrous zirconia and activated carbon by the post-synthesis method followed by thermal treatment at 300 ^oC, and they evaluated the acid catalytic activity of these four supported $H_3PW_{12}O_{40}$ by the transesterification of canola oil containing 10 wt.% oleic acid under the conditions of 200 ^oC and 600 psi. It is found that $H_3PW_{12}O_{40}/ZrO_2$ with $H_3PW_{12}O_{40}$ loading of 10 wt.% exhibited the highest FAME yields, attributed to the contribution of both Brønsted and Lewis acid sites of the supported catalysts.[99] This group also found that the solid acid catalyst prepared by impregnation of $H_3PW_{12}O_{40}$ on Nb_2O_5 support was also an eminent candidate for biodiesel production from used cooking oil with 8% FFAs content.[101] The maximum FAME yield (92 %) was obtained by using $H_3PW_{12}O_{40}/Nb_2O_5$ with $H_3PW_{12}O_{40}$ loading of 25 wt.% under the optimized conditions of 200 ^oC, 600 psi, methanol-to-oil molar ratio of 8: 1 and 3 wt.% catalyst loading in 20 h. Good catalytic activity and reusability of supported HPAs solid acids were as well verified by Kozhevnikov and Dias.[100,103] However, the aforementioned supported HPAs were prepared by a post-synthesis grafting route, and the method suffers from drawbacks of poor control over HPA loading, HPA leaching and the loss of homogeneity due to minor changes in the structure. All of these may lead to reduced catalytic activity of the immobilized HPA catalysts.[110] The problems can be solved by using one step sol–gel co-condensation technique, which will be discussed in detail in section 3.2.

3.1.6 H-form zeolites

Zeolites are microporous crystalline solids with well-defined structures containing Al, Si and O in their framework and cations. Zeolites have found wide application in oil refining, petrochemistry and in the production of fine chemicals. Their success is based on the possibility to prepare zeolites with strong Brønsted acidity (also including Lewis acid sites) that can be controlled within a certain range, combined with a good resistance to high reaction temperatures. However, diffusion of the reactant molecules to the active sites of zeolites can become a limiting process due to their small pore size (lower than 2 nm). In the production of biodiesel, H^+ ion exchanged acid form zeolites such as H-ZSM-5, H-MOR, H-BETA and H-USY are found showing poor esterification or transesterification catalytic activity that is explained by internal diffusion limitations of the bulky reactant molecules into the micropores of zeolites. Consequently, esterification or transesterification takes place only at the external surface of zeolites.[16,55] Therefore, zeolites with small pores are not suitable for biodiesel manufacture because of the serious diffusion limitations of the bulky FFA or TG molecules.

3.1.7 Acidic ILs and immobilized ILs

ILs have received extensive attention because of their special properties such as negligible volatility, remarkable solubility, no corrosion and the variety of structures available, and they could be used as dual solvents and catalysts.[111,112] Various $–SO_3H$ functionalized strong Brønsted acidic ILs, *e.g.* N-methyl-2-pyrrolidonium methyl sulfonate ([NMP][CH_3SO_3]), $[(CH_2)_4SO_3HPy][HSO_4]$ and 1-(3-sulfonic acid) propyl-3-methylimidazolium hydrogen sulfate ($[C_3SO_3H\text{-}mim]HSO_4$), have received much attention for their potential applications in replacement of conventional homogeneous or heterogeneous acid catalysts because they are very effective for many acid-catalyzed reactions including esterification and transesterification (Table 5), and they have activities comparable to those of homogeneous catalysts (*e.g.* sulfuric acid).[113–118] The ILs also suffer from some drawbacks such as limited solubility with organic compounds, especially polar molecules, which not only cause catalyst loss but also add purification difficulties. In addition, the high viscosity of the ILs increases the mass-transfer resistance and limits their industrial application. The problems are attempted to be solved by immobilization of acidic ILs on porous silica,[119] polystyrene-based polymers[120] or poly(divinylbenzene) (PDVB) support.[114] For examples, Liang reported that PDVB supported $[SO_3H(CH_2)_3VPy]HSO_4$ material showed high activities for one-pot biodiesel synthesis from cooking oil with a high FFA content at 70 °C, and a total yield of biodiesel reached 99.1% over period of 12 h.[114] After the reactions, the solid PDVB-$[SO_3H(CH_2)_3VPy]HSO_4$ catalyst was recovered easily by filtration for the next catalytic cycle. It is found that a yield of 99% was obtained even after the catalyst had been recycled six times. This excellent catalytic stability of PDVB-$[SO_3H(CH_2)_3VPy]HSO_4$ is explained in terms of its hydrophobic surface and stable porous structure of the immobilized ILs. In order to further improve the esterification activity of the supported Brønsted acidic ILs, Karimi's group recently developed a hydrophobic IL, *i.e.* 1-methyl-3-octylimidazolium hydrogen sulfate ($[MOIm]HSO_4$) comprising Brønsted acid anions inside the mesochannels of SBA-15-functionalized propylsulfonic acid (SBA-15-Pr-SO_3H), and the resulting $[MOIm]HSO_4$@SBA-15-Pr-SO_3H catalyst showed significantly higher catalytic activity than that of $[MOIm]HSO_4$ or SBA-15-Pr-SO_3H in direct esterification of carboxylic acids at ambient temperature under solvent-free conditions. The result clearly highlights the existence of a synergistic effect between grafted sulfonic acid groups and the immobilized $[MOIm]HSO_4$ IL system: the hydrophobic nature of $[MOIm]HSO_4$ afforded paths for efficient mass transfer of starting materials to the active sites, while the acid site cooperativity led to the enhanced Brønsted acid strength of the $[MOIm]HSO_4$@SBA-15-Pr-SO_3H catalyst. The prepared solid IL can be reused at least 4 reaction runs without significant activity loss.[121] Additionally, silica supported HPA ($H_4SiW_{12}O_{40}$)-based IL (SWIL/SiO_2) catalysts, with different contents of SWIL were prepared by Li's group through a free radical addition reaction between allyl groups of SWIL and sulfhydryl groups of sulfhydryl functionalized SiO_2, and the catalytic activity and reusability of the catalysts were evaluated through esterification of oleic acid with methanol at 100 ^oC. It showed that the fresh SWIL/SiO_2 had high catalytic activity close to that of SWIL and could be easily separated from the reaction system by simple filtration. However, the leaching of SWIL in the esterification reaction caused the deactivation of SWIL/SiO_2.[122] More recently, Xiao's group developed an interesting heterogeneous IL catalyst, *i.e.* $SO_3CF_3^-$ anion-functionalized mesoporous copolymer PDVB-[C_1vim][SO_3CF_3] (C_1 = CH_3, vim = 1-vinylimidazolate, Fig. 8). This catalyst

Table 5 Recent typical examples on the use of acidic ionic liquids in biodiesel production

Catalyst	Biodiesel production					Ref
	Preparation method	Feedstocks	Reaction conditions	Activity	Recyclability	
PDVB-$[SO_3H(CH_2)_3VPy]HSO_4$	Copolymerization of DVB with $[SO_3H(CH_2)_3VPy]HSO_4$ oligomers	Cooking oil containing 22 wt.% of FFAs (esterification and transesterification)	Waste oil 5 g; Methanol 2.91 g; 70 °C; 12 h; Catalyst amount 1 wt.% (referred to waste oil)	Total yield of biodiesel (%) = 99	No catalytic activity loss after recycling six times	[114]
$[MOIm]HSO_4$@SBA-15-Pr-SO_3H	Post-synthesis	Acetic acid (esterification)	1-octanol-to-acetic acid molar ratio = 1: 1.6; Room temperature; 40 h; Catalyst amount 10 mol.%	Yield (%) = 93	No catalytic activity loss after recycling four times	[121]
$[(CH_2)_4SO_3HPy][HSO_4]$	Two-step synthesis	Cottonseed oil Methanol (transesterification)	Methanol-to-oil molar ratio = 12: 1; 170 °C, 5 h; Catalyst amount 2 wt.% (referred to cottonseed oil)	Yield (%) = 92	Not studied	[127]
PDVB-$[C_1vim][SO_3CF_3]$	Anion-exchange	Tripalmitin Methanol (transesterification)	Methanol-to-tripalmitin molar ratio = 89: 1; 65 °C; 16 h; Catalyst amount 5 wt. % (referred to tripalmitin);	Yield (%) = 97	No obvious activity loss after recycling four times	[123]
$[MIMPS]_3PW_{12}O_{40}$ $[PyPS]_3PW_{12}O_{40}$ $[TEAPS]_3PW_{12}O_{40}$	Two-step synthesis	Citric acid	n-butanol-to-citric acid molar ratio = 5: 1; 130 °C; 3 h; Catalyst amount 0.2 mol.% (referred to citric acid);	Yield (%) = 95 Yield (%) = 91 Yield (%) = 89	A slight decrease in the catalytic activity of the recovered catalyst was found after the fourth reaction	[124]

exhibited much higher activity in transesterification of tripalmitin with methanol in comparison with the corresponding homogeneous $[C_1vim][SO_3CF_3^-]$ as well as SBA-15-$[C_1vim][SO_3CF_3]$ and Amberlyst-15 under the conditions of methanol-to-tripalmitin molar ratio 89: 1 and 65 °C. Moreover, the new heterogeneous IL catalyst showed very good recyclability, and no obvious activity loss was found after recycling four times. The authors explain that the excellent catalytic performance of ILs functionalized on the PDVB-vim support is strongly related to the unique features of high enrichment and good miscibility of the superhydrophobic mesoporous polymers for the reactants, encouraging the design and development of a wide variety of catalysts with both high catalytic activity and good recyclability for the conversion of organic compounds.[123]

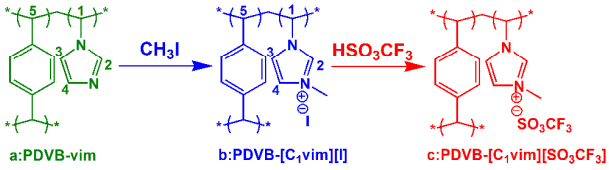

Fig. 8 Procedure of the synthesis of PDVB-$[C_1vim][SO_3CF_3]$ from PDVB-vim. (Adapted from ref. 123 with permission from ACS.)

Wang's group synthesized a series of HPA-based ILs, *e.g.* $[MIMPS]_3PW_{12}O_{40}$, $[PyPS]_3PW_{12}O_{40}$ and $[TEAPS]_3PW_{12}O_{40}$, and the materials are composed of three propane sulfonate (PS) functionalized organic cations and one inorganic heteropolyanion (Fig. 9). They were used as "reaction-induced self-separation catalysts" for various esterification reactions with one of the reactants being polycarboxylic acid or polyol. The good solubility in the polycarboxylic acid or polyol, nonmiscibility with ester product and high melting points of the HPA-based IL catalysts resulted in the switching from homogeneous to heterogeneous catalysis, which made the recovery and catalytic reuse of this kind of catalyst very convenient. The catalyst can be recycled without any regeneration steps, and only a slight decrease in the catalytic activity of the recovered catalyst was found after the fourth reaction. The authors also found that it was the functional group PS in the IL catalysts rather than the heteropolyanion that provided the acid site responsible for the high esterification reactivity.[124]

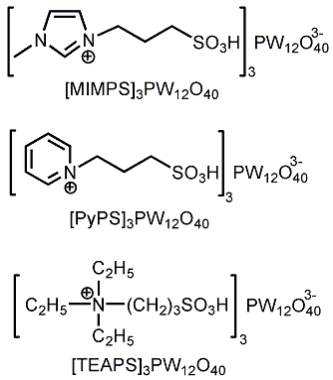

Fig. 9 HPA-based ILs: $[MIMPS]_3PW_{12}O_{40}$ (a); $[PyPS]_3PW_{12}O_{40}$ (b) and $[TEAPS]_3PW_{12}O_{40}$ (c). (Adapted from ref. 124 with permission from Wiley-VCH.)

3.2 Porosity and surface hydrophobicity of the catalyst

Owing to unsatisfactory catalytic activity in esterification and transesterification at atmosphere refluxing temperature of alcohol, most of the aforementioned solid acid-catalyzed biodiesel synthesis processes, especially for the transesterification, proceeded at higher temperature and higher pressure as well as higher methanol-to-oil molar ratio and longer reaction time, which made the processes uneconomic and thereby limiting the practical applications of solid acids for biodiesel production. The heterogeneous catalytic activity and stability of the solid acids can be improved further by adjusting their porosity (or textural property) and surface hydrophobicity/hydrophilicity balance, accordingly, biodiesel production processes may carry out under mild conditions.

On the one hand, to a great extent, the catalytic activity of the solid catalysts is determined by their textural and morphological properties. Porous materials, especially mesoporous materials with unique surface physicochemical properties, have been successfully applied in many liquid phase catalytic processes.[110,125,126] Therefore, rationally designed novel solid acid catalysts with perfect porous structure including uniform pore channel, large pore diameter, large surface area and high pore volume can increase the active site numbers and the accessibility of active sites on a given catalysts surface and inside the pores to the substrates as well as decrease the mass-transport limitation of the reactant or product molecules, which in turn enhance the catalytic activity of biodiesel production. This research topic is of paramount importance for both academia and chemical industry.[127,128]

Microporous materials such as zeolites with pore diameters in the range of one or two nanometers are limited to accommodate bulky and viscous C_{12}–C_{22} TGs or FFAs molecules to their pores due to severe mass-transport problem. Mesoporous (pore diameters lie in the range of two to fifty nanometers) and macroporous (pore diameters are larger than fifty nanometers) materials are the first choice for catalytic processes involving large molecules, which allow diffusion of liquid to the active centres within the regular internal channels of the materials. Relying on sol–gel, solution and surface chemistry, there is great potential to explore novel strategies for mesoporous catalytic materials.[129] Generally, two routes, post-synthesis grafting and sol–gel co-condensation, are applied to incorporate acid sites onto various mesoporous supports such as silica (*e.g.* SBA-12, -15 and -16; MCM-41 and -48; KIT-6; FDU), carbon (*e.g.* CMK-1, -3 and -5), PMO and acidic metal oxides (*e.g.* ZrO_2, TiO_2, Nb_2O_5 and Ta_2O_5). Grafting the active components onto porous materials is a standard method of preparation of hybrid porous catalytic materials. Nevertheless, post-synthesis grafting route has the drawbacks of poor control over loading (variable and often low levels are achieved), acid site leaching and the loss of homogeneity due to minor changes in the structure. All of these may lead to reduced activity of the immobilized acid catalysts.[110] The problems can be solved by using one step sol–gel co-condensation technique. This emerging approach to the incorporation of chemical functionalities into porous materials is based on the *in situ* incorporation of the functionalities during the sol–gel process. The novel route leads to mesoporous solids with a more homogeneous distribution of the active phase throughout the structure of the porous materials; moreover, the hydrolytic

sol–gel process can improve the interaction between the acid sites and the support during the hydrolysis and condensation steps, and thereby the stability of the catalysts obtained is improved owing to the reduced leaching of the active phase.[130–132] Successful examples are described below.

Usually, mesoporous HPA-based hybrid catalysts are obtained by sol–gel inclusion of HPAs in mesoporous silica walls. These materials feature a HPAs/SiO_2 framework and have high surface area and regular pore structure.[133] However, HPAs interact weakly with the silica matrix, and therefore they can easily leach out when a polar solvent or reactant is used;[134] additionally, silica is nonacidic, and the overall acid catalytic activity of HPAs/SiO_2 originates from HPAs only. Both of the drawbacks decrease tremendously the applicability of these materials in heterogeneous acid catalysis. In the search for sustainable, effective and robust HPA-based catalysts for biodiesel production, a series of $H_3PW_{12}O_{40}/Ta_2O_5$ and $H_3PW_{12}O_{40}/ZrO_2$ composite catalysts with 3D interconnected sponge-like mesostructure were developed by one step template-assisted sol–gel co-condensation technique. In the $H_3PW_{12}O_{40}/Ta_2O_5$ or $H_3PW_{12}O_{40}/ZrO_2$ catalysts, Ta_2O_5 or ZrO_2 can act as both the acid site and the support. It has been studied that Ta_2O_5 or ZrO_2 exhibits both Brønsted and Lewis acidity, and they have been used in some acid-catalyzed reactions including esterification, alkylation and isomerization.[45,135,136] Additionally, Ta^{5+} (1.50, 0.064 nm) or Zr^{4+} ion (1.33, 0.072 nm) and W^{6+} ion (1.70, 0.060 nm) have well-matched electronegativity and ionic radius. Thus, the terminal W=O groups within the Keggin units interact to the surface ≣TaOH or ≡ZrOH groups within the Ta_2O_5 or ZrO_2 support *via* W–O–Ta(Zr) covalent bindings and form (≣$TaOH_2)_n^+[H_{3-n}PW_{12}O_{40}]^{n-}$ or (≡$ZrOH_2)_n^+[H_{3-n}PW_{12}O_{40}]^{n-}$ species at the interface of the composites catalysts. The species can enhance the interaction between the heteropolyanions ($PW_{12}O_{40}^{3-}$) and hence the formation of larger polyanions. Larger heteropolyanions can effectively delocalize the negative charge required for the formation of Brønsted acid centers and promote the release of protons, ultimately leading to enhanced Brønsted acidity of $H_3PW_{12}O_{40}/Ta_2O_5$ or $H_3PW_{12}O_{40}/ZrO_2$ with respect to bulk $H_3PW_{12}O_{40}$.[99,137] Meanwhile, this strong interaction effectively inhibited the loss of the Keggin unit during the preparation procedure, and therefore, $H_3PW_{12}O_{40}$ loading in the composite catalysts are controllable. At the same $H_3PW_{12}O_{40}$ loading (*ca*. 11 wt.%), $H_3PW_{12}O_{40}/Ta_2O_5$ exhibited enhanced catalytic activity in esterification of lauric acid and transesterification of tripalmitin or soybean oil (in the presence of 20 wt.% of myristic acid) with methanol under mild conditions (*i.e.* atmosphere refluxing temperature of methanol) in comparison to as-prepared SBA-15 silica supported $H_3PW_{12}O_{40}$. After the esterification reaction proceeded for 3 h, the yield of ethyl laurate reached 65.6 and 20.0%, respectively, for $H_3PW_{12}O_{40}/Ta_2O_5$ and $H_3PW_{12}O_{40}$/SBA-15; additionally, over period of 6 h, the yield of methyl palmitate was 51.4 and 9.8%, respectively, for $H_3PW_{12}O_{40}/Ta_2O_5$ and $H_3PW_{12}O_{40}$/SBA-15. The results confirm that the enhanced acidity originating from the synergistic effect between $H_3PW_{12}O_{40}$ and Ta_2O_5 play a paramount role to the excellent esterification and transesterification reactivity. Additionally, although wormhole-like mesoporous $H_3PW_{12}O_{40}/Ta_2O_5$ is disordered, the characteristics of these catalysts including uniform pores, high surface areas and homogeneous dispersion of the Keggin unit throughout the catalysts give a positive contribution to this enhanced catalytic activity. Importantly, leaching of $H_3PW_{12}O_{40}$ into the reaction media was inhibited effectively, and the $H_3PW_{12}O_{40}/Ta_2O_5$ can restore its catalytic activity after five consecutive runs through suitable regeneration method. The result further confirms that one step co-condensation route and strong interaction between the Keggin unit and Ta_2O_5 support ensure the $H_3PW_{12}O_{40}/Ta_2O_5$ highly catalytic stability. The excellent catalytic activity and stability of $H_3PW_{12}O_{40}/Ta_2O_5$ may offer it good opportunities in biodiesel production.[138]

On the other hand, adsorption and desorption are the key catalytic steps of a solid catalyst, which are determined by its surface hydrophobicity and hydrophilicity. Esterification of FFAs and transesterification of TGs involve hydrophobic reactants (*e.g.* TGs or FFAs) and hydrophilic products (*e.g.* water or glycerol). For the esterification reaction, the presence of significant quantities of water in the reaction system inhibits FFAs from approaching the active sites effectively, and thereby slowing down the esterification reaction rate. This effect is exacerbated if the solid acids (*e.g.* Zr–SBA-15, SO_4^{2-}/ZrO_2, $H_3PW_{12}O_{40}/Ta_2O_5$ or $H_3PW_{12}O_{40}/ZrO_2$) are surface hydrophilic. For the transesterification reaction, the strong adsorption of the hydrophilic glycerol product on the surface of hydrophilic catalyst severely limits the adsorption and diffusion of hydrophobic TG reactants within the channels of the catalyst, leading to poor transesterification reactivity of the catalysts; meanwhile, this strong adsorption of glycerol on the surface of hydrophilic catalyst results in catalyst deactivation in some extents, which has been found during the process of recycling uses of the catalyst. Therefore, tuning the surface hydrophilic/hydrophobic balance of the catalysts is also necessary to optimize the adsorption and desorption steps and thus the overall biodiesel synthesis processes. Generally, tuning the porosity and surface hydrophilic/hydrophobic balance of the solid acids can be realized simultaneously by the incorporation of hydrophobic alkyl groups-containing organosilica moieties into the catalysts. By the combination of strong acidity, well-defined mesoporosity and increased surface hydrophobicity, as-designed organic-inorganic hybrid catalysts exhibit excellent catalytic performance in biodiesel synthesis. Moreover, it is found that pore morphologies, porosities and surface hydrophilicity/hydrophobicity influence the acid catalytic performance of the hybrid acid catalysts obviously. The successful examples are described below.

Zirconium-containing periodic mesoporous organosilicas (Zr–PMOs) with varying framework organic content have been demonstrated through a direct synthesis method by using different ratios of tetraethyl orthosilicate (TEOS) and 1,4-bis-(triethoxysilyl)benzene (BTESB) silicon precursors. Compared with zirconium-containing SBA-15 silica (Zr–SBA-15), the strong hydrophobic character of organosilicon species in Zr–PMOs hybrid catalysts leads to an impressive beneficial effect on the intrinsic catalytic activity of the zirconium sites in biodiesel production by the simultaneous esterification of FFAs and transesterification of TGs contained in crude palm oil with methanol under the conditions of 209 °C, methanol-to-palm oil

molar ratio of 48.5: 1 and catalyst loading 12.8 wt.%

Table 6 Novel hybrid solid acid catalysts with improved porosity and/or surface hydrophobicity in biodiesel production[a]

Catalyst	Biodiesel production							Refs
	Feedstocks	Reaction conditions	Activity				Recyclability	
Zr–PMOs	Crude palm oil (simultaneous esterification and transesterification)	Methanol-to-oil molar ratio = 48.5; 1; 209 °C; 6 h; Catalyst amount 12.8 wt.% (referred to oil)	Yield (%) of methyl esters = 80–85%				Negligible activity loss after two cycles	[139]
	Eruca sativa Gars oil (transesterification)	Methanol-to-oil molar ratio = 90: 1; 65 °C; atmospheric pressure; 24 h; Catalyst amount 5 wt.%;	MP (%)	MS (%)	MO (%)	ML (%)	Negligible activity loss after three cycles	[140,141]
SO_4^{2-}/ZrO_2 (calcined at 600 °C)			26	28	20	29		
$SO_4^{2-}/ZrO_2–SiO_2$(Et)-3D_{int}			82	88	65	73		
$SO_4^{2-}/ZrO_2–SiO_2$(Ph)-2D_{hex}			100	100	100	91		
$SO_4^{2-}/ZrO_2–SiO_2$(Ph)-3D_{cub}			83	84	78	92		
$SO_4^{2-}/ZrO_2–SiO_2$(Et)-3D_{cub}			80	79	75	69		
	Soybean oil-containing 20 wt.% of myristic acid (simultaneous esterification and transesterification)	Methanol-to-oil molar ratio = 90: 1; 65 °C and atmospheric pressure; Catalyst amount = 2 wt.%; $H_3PW_{12}O_{40}$ loading (wt.%) = 10	MM (%)	MP[d] (%)	MS[d] (%)	ML[d] (%)	No obvious activity loss after four cycles	[142,143,145]
$H_3PW_{12}O_{40}/Ta_2O_5$-3D_{int}			55[b]	25	20	30		
$H_3PW_{12}O_{40}/Ta_2O_5–Si$(Me)-3$D_{int}$			79[b]	66	54	81		
$H_3PW_{12}O_{40}/Ta_2O_5–Si$(Ph)-3$D_{int}$			70[b]	41	35	52		
$H_3PW_{12}O_{40}–Ta_2O_5$/Si(Et)Si-3D_{int}			100[c]	84	69	100		
$H_3PW_{12}O_{40}–Ta_2O_5$/Si(Ph)Si-3D_{int}			100[c]	73	62	100		
$H_3PW_{12}O_{40}/ZrO_2$-3D_{int}	Levulinic acid (LA) (esterification)	Methanol-to-LA molar ratio = 7: 1 65 °C; atmospheric pressure; 2 h; Catalyst amount 2wt.% $H_3PW_{12}O_{40}$ loading (wt.%) = 7	Yields (%) of methyl levulinate = 45				No obvious activity loss after three cycles	[144,147]
$H_3PW_{12}O_{40}/ZrO_2–Si$(Ph)-3$D_{int}$			Yields (%) of methyl levulinate = 59					
$H_3PW_{12}O_{40}/ZrO_2–Si$(Ph)Si-3$D_{int}$			Yields (%) of methyl levulinate = 76					
$H_3PW_{12}O_{40}/ZrO_2–Si$(Ph)Si-2$D_{hex}$			Yields (%) of methyl levulinate = 90					
$H_3PW_{12}O_{40}/ZrO_2–Si$(Et)Si-3$D_{int}$			Yields (%) of methyl levulinate = 58					

[a] All hybrid catalysts presented were prepared by a sol-gel co-condensation method. MP: methyl palmitate (C16:0); MS: methyl stearate (C18:0); MO: methyl oleate (C18:1); MM: methyl myristate (C14:0); ML: methyl lioleate (C18:2).
[b] MM was obtained by esterification of myristic acid with methanol for 30 min.
[c] MM was obtained by esterification of myristic acid with methanol for 60 min.
[d] MP, MS and ML were obtained by transesterification of soybean oil with methanol for 24 h.

(referred to oil). Moreover, the catalytic activity of the highly hybridized materials is hardly affected in presence of large amounts of water, confirming their very good water tolerance; additionally, the materials can be used two times without activity loss (Table 6).[139]

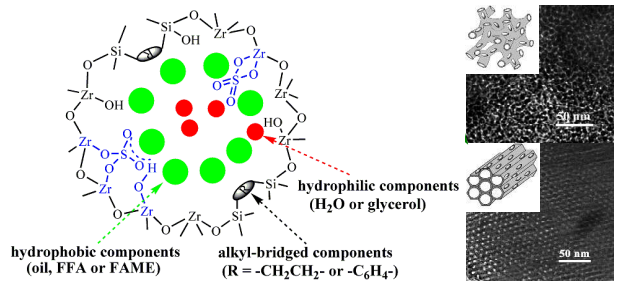

Fig. 10 Wall structure, morphology of 2D hexagonal *p6mm* and 3D interconnected worm-hole-like SO_4^{2-}/ZrO_2–SiO_2(Et/Ph) hybrid catalyst and schematic representation of preferential adsorption of oily hydrophobic species on the hybrid catalyst surface.

SO_4^{2-}/ZrO_2 is conventionally prepared by a post-synthesis grafting method followed by calcination at approximately 600 °C. However, the method results in SO_4^{2-}/ZrO_2 with poor porosity and thereby limiting its catalytic activity; meanwhile, sulfate group leaching in liquid phase catalysis occurs and thereby decreasing the reusability of the catalyst. Functionalization of SO_4^{2-}/ZrO_2 by alkyl-bridged organosilica moieties ($O_{1.5}$–Si–R–Si–$O_{1.5}$, where R = $–CH_2CH_2–$ or $–C_6H_4–$) can improve the porosity, tune structural orderings and pore geometries as well as increase the surface hydrophobicity of SO_4^{2-}/ZrO_2 simultaneously, leading to the SO_4^{2-}/ZrO_2–SiO_2(R) hybrid materials with enhanced catalytic activity and stability towards the esterification and transesterification reactions.[47,140] It should be noted that the single step sol–gel co-condensation technique combined with low temperature (100 °C) hydrothermal treatment, rather than post-synthesis grafting route, was applied to prepare the SO_4^{2-}/ZrO_2–SiO_2(R) hybrid materials. By using this strategy, strong interaction between SO_4^{2-}/ZrO_2 and organosilica framework as well as homogeneous dispersion of SO_4^{2-}/ZrO_2 throughout the hybrid catalyst were also obtained. This one step preparation process included co-hydrolysis and -condensation of zirconium precursor (*i.e.,* Zr(*n*-OBu)$_4$) and bissilylated organic precursor 1,2-bis-(trimethoxysilyl)ethane (BTMSE) or BTESB in the presence of $(NH_4)_2SO_4$ and nonionic surfactant P123 or F127 under an acidic condition (pH < 1), followed by subsequent hydrothermal treatment and dehydration. Owing to obviously slower hydrolysis rate of BTMSE or BTESB with respect to Zr(*n*-OBu)$_4$, prehydrolysis of BTMSE or BTESB at 40 °C for 1 h was proceeded at the beginning of the material preparation. This hydrolysis rate matching between BTMSE (or BTESB) and Zr(*n*-OBu)$_4$ ensure the –Si–C–Si– units were successfully introduced as bridging components directly into ZrO_2 framework through –Zr–O–Si–C–Si–O– linkages (Fig. 10). Moreover, structural ordering- and pore geometry-controlled fabrication of mesostructured SO_4^{2-}/ZrO_2–SiO_2(R) materials with two-dimensional (2D) hexagonal *p6mm*, three-dimensional (3D) cubic *Im3m* and 3D interconnected wormhole-like pore morphologies were successfully realized by selecting suitable bissilylated organic precursors, nonionic surfactants and the initial Si/Zr molar ratio. For examples, P123-directed, benzene-bridged hybrid materials obtained at initial Si/Zr molar ratio of 0.4–1.0 exhibited ordered 2D hexagonal *p6mm* structure (SO_4^{2-}/ZrO_2–SiO_2(Ph)-2D_{hex}), while P123-directed, ethane-bridged hybrid materials obtained under the same conditions possessed disordered 3D interconnected wormhole-like pore morphologies (SO_4^{2-}/ZrO_2–SiO_2(Et)-3D_{int}). Additionally, F127-directed, benzene- or ethane-bridged hybrid materials obtained at initial Si/Zr molar ratio of 1.0 showed ordered 3D cubic *Im3m* structure (SO_4^{2-}/ZrO_2–SiO_2(Ph)-3D_{cub} or SO_4^{2-}/ZrO_2–SiO_2(Et)-3D_{cub}). At atmosphere refluxing temperature of methanol (65 °C), as-prepared multifunctionalized SO_4^{2-}/ZrO_2–SiO_2(R) materials exhibited enhanced catalytic activity in transesterification of tripalmitin and low-cost virgin plant oil, *Eruca Sativa Gars* (ESG) oil with methanol in comparison with SO_4^{2-}/ZrO_2; moreover, the catalytic activity of the SO_4^{2-}/ZrO_2–SiO_2(R) was significantly influenced by their structural orderings and pore geometries. Ordered 2D hexagonal mesostructured SO_4^{2-}/ZrO_2–SiO_2(Ph) material exhibited considerably higher catalytic activity with respect to 3D cubic or 3D worm-hole-like SO_4^{2-}/ZrO_2–SiO_2(Ph) materials at the same S/Zr and Si/Zr molar ratios (Table 6).[141]

The enhanced catalytic activity of SO_4^{2-}/ZrO_2–SiO_2(R) with respect to SO_4^{2-}/ZrO_2 is due to a combination of well-defined mesoporosity and increased surface hydrophobicity except for the inherent strong acidity of SO_4^{2-}/ZrO_2 itself. SO_4^{2-}/ZrO_2 exhibits poor porosity with small BET surface area (12 $m^2\ g^{-1}$), however, the BET surface area is enlarged significantly after introduction of ethane- or benzene-bridged organosilica moieties ($O_{1.5}$–Si–CH_2CH_2–Si–$O_{1.5}$ or $O_{1.5}$–Si–C_6H_4–Si–$O_{1.5}$) into the framework of SO_4^{2-}/ZrO_2. For example, the BET surface area of SO_4^{2-}/ZrO_2–SiO_2(Ph)-2D_{hex}, SO_4^{2-}/ZrO_2–SiO_2(Et)-3D_{int} and SO_4^{2-}/ZrO_2–SiO_2(Ph)-3D_{cub} obtained at Si/Zr molar ratio of 1.0 is 360, 270 and 108 $m^2\ g^{-1}$, respectively.[134] Thus, more acid sites can be provided for esterification or transesterification reactions. SO_4^{2-}/ZrO_2–SiO_2(Ph)-2D_{hex} can give rise to the highest population of available acid sites; meanwhile, its highly ordered mesostructure would minimize diffusion problems of bulky alkyl chain molecules. Therefore, it exhibits the highest catalytic activity among the aforementioned three SO_4^{2-}/ZrO_2–SiO_2(Ph) catalysts. On the other hand, the enhanced surface hydrophobicity of the SO_4^{2-}/ZrO_2–SiO_2(R) can create an unsuitable environment for the hydrophilic products (*e.g.* water or glycerol) selectively, leading to easy desorption of them from the catalyst surface; meanwhile, the acid site deactivation due to the strong adsorption of water or glycerol on the catalyst surface is inhibited (Fig. 10). As a consequence, SO_4^{2-}/ZrO_2–SiO_2(R)-catalyzed esterification or transesterification reactions can carry out at a faster rate. Except for the enhanced catalytic activity, the one-pot preparation route can effectively inhibit the loss of SO_4^{2-} ion during recycling the catalysts, and the hybrid catalysts can be used at least three times without obvious activity loss (Fig. 11). Therefore, as-prepared SO_4^{2-}/ZrO_2–SiO_2(R) materials can be regarded as the promising heterogeneous acid catalyst candidates for biodiesel production from low quality biomass under mild conditions.

Similarly, in order to further improve the heterogeneous acid catalytic activity and avoid deactivation of the $H_3PW_{12}O_{40}/ZrO_2$ and $H_3PW_{12}O_{40}/Ta_2O_5$, the hydrophobic alkyl groups were introduced into these composite catalysts by the following two

strategies. One strategy to prepare mesostructured ZrO_2- or Ta_2O_5-based hybrid catalysts functionalized by both alkyl group R (R = $–CH_3$ or $–C_6H_5$) and the Keggin-type HPA (*e.g.* $H_3PW_{12}O_{40}/ZrO_2–Si(R)$ or $H_3PW_{12}O_{40}/Ta_2O_5–Si(R)$, Fig. 12a) is incorporation of alkyl groups terminally bonded on the ZrO_2 or Ta_2O_5 framework *via* (Zr)Ta–O–Si–C linkage. In this manner, one-pot template-assisted sol–gel co-condensation–hydrothermal treatment route was designed, and the alkyl groups were provided by terminal-silylated organic precursor such as methyltrimethoxysilane (MeTMS) or phenyltrimethoxysilane (PhTMS).[142–144] Additionally, by replacement of alkyltrimethoxysilane with bissilylated organic precursor (*e.g.* BTMSE or BTESB), the alkyl-bridged organosilica moieties were directly introduced into the framework structure of $H_3PW_{12}O_{40}/ZrO_2$ and $H_3PW_{12}O_{40}/Ta_2O_5$ through (Zr)Ta–O–Si–C–Si covalent bonds using the aforementioned route (Fig. 12b). Since the ethane- or benzene-bridged organosilica groups (*i.e.* $O_{1.5}–Si–CH_2CH_2–Si–O_{1.5}$ or $O_{1.5}–Si–C_6H_4–Si–O_{1.5}$) are structural components of the framework of the prepared $H_3PW_{12}O_{40}–ZrO_2/Si(R)Si$ or $H_3PW_{12}O_{40}–Ta_2O_5/Si(R)Si$ hybrid catalysts, unique physicochemical characteristics such as 3D interconnected mesoporosity and enhanced surface hydrophobicity of the catalysts can be obtained. As a consequence, the promising candidates for the creation of efficient heterogeneous acid catalyst towards biodiesel production were obtained.[144–147]

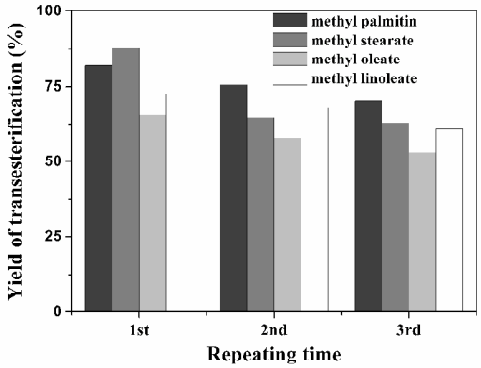

Fig. 11 Recyclability of the SO_4^{2-}-1.2/ZrO_2–SiO_2(Et) material in transesterification of ESG oil with methanol. Catalyst amount 5 wt.%; 24 h; 65 °C. (Adapted from ref. 47 with permission from Wiley-VCH.)

The heterogeneous acid catalytic activity of alkyl-free $H_3PW_{12}O_{40}/Ta_2O_5$ and phenyl or methyl groups terminally bonded $H_3PW_{12}O_{40}/Ta_2O_5–Si(Ph)$ or $H_3PW_{12}O_{40}/Ta_2O_5–Si(Me)$ towards biodiesel production from soybean oil in the presence of 20 wt.% myristic acid was compared under the conditions of 2 wt.% catalyst loading and methanol refluxing temperature (65 °C). For the $H_3PW_{12}O_{40}/Ta_2O_5$-, $H_3PW_{12}O_{40}/Ta_2O_5–Si(Ph)$- and $H_3PW_{12}O_{40}/Ta_2O_5–Si(Me)$-catalyzed myristic acid esterification reaction, the yield of methyl myristate reached 54.8, 70.2 and 79.4%, respectively, after the reaction proceeded for only 30 min. As for the aforementioned three hybrid materials-catalyzed soybean transesterification reaction, three main FAMEs were detected, and they were methyl palmitin, methyl oleate and methyl linoleate. Three hybrid materials followed the transesterification activity order $H_3PW_{12}O_{40}/Ta_2O_5$ < $H_3PW_{12}O_{40}/Ta_2O_5–Si(Ph)$ < $H_3PW_{12}O_{40}/Ta_2O_5–Si(Me)$, in line with their esterification activity. For the most active $H_3PW_{12}O_{40}/Ta_2O_5–Si(Me)$-catalyzed soybean oil transesterification activity, the yield of methyl palmitin, methyl oleate and methyl linoleate were 65.9, 53.9 and 81.2%, respectively, over period of 24 h (Table 6).[143]

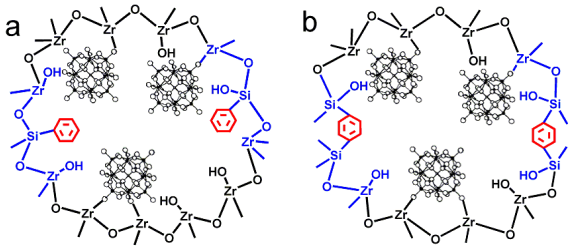

Fig. 12 Wall structure of benzene-terminally bonded $H_3PW_{12}O_{40}/ZrO_2–Si(Ph)$ (a) and benzene-bridged $H_3PW_{12}O_{40}/ZrO_2–Si(Ph)Si$ (b) hybrid catalysts.

For the mesostructured ZrO_2- or Ta_2O_5-based hybrid catalysts functionalized by both alkyl-bridged organosilica moieties and the Keggin-type HPA, they also exhibited enhanced esterification and transesterification activity in comparison to $H_3PW_{12}O_{40}/ZrO_2$ or $H_3PW_{12}O_{40}/Ta_2O_5$. Moreover, the contents of alkyl-bridged organosilica moieties in the hybrid catalysts influenced the catalytic activity obviously since alkyl-bridged organosilica moieties affected the porosity and surface hydropobicity of the hybrid catalysts. For example, in the $H_3PW_{12}O_{40}–Ta_2O_5/Si(Et)Si$-catalyzed transesterification of soybean oil in the presence of 20 wt.% myristic acid system, under the condition of 2 wt.% catalyst loading and methanol refluxing temperature (65 °C), the yields of FAMEs including methyl palmitin, methyl oleate and methyl linoleate increased with the content of ethane-bridged organosilica group from 0 to 20 mol%; however, further increasing the concentration of ethane-bridged organosilica group to 80 mol%, the yields of each FAME decrease gradually.[145] Similar results were also found in the $H_3PW_{12}O_{40}–ZrO_2/Si(Et)Si$-catalyzed transesterification of ESG oil. For example, under the conditions of 5 wt.% catalyst loading, 24 h and methanol refluxing temperature (65 °C), the yields of methyl palmitate, methyl stearate, methyl oleate, and methyl lioleate reached 99.9, 67.8, 73.5, and 75.3%, respectively, for the $H_3PW_{12}O_{40}–ZrO_2/Si(Et)Si$ with ethane-bridged organosilica group percentage of 60 mol%. Under the same conditions, the yields of methyl palmitate, methyl stearate, methyl oleate and methyl lioleate were 35.2, 18.4, 18.9 and 17.5%, respectively, for the $H_3PW_{12}O_{40}/ZrO_2$.[146]

The enhanced esterification and transesterification reactivity of $H_3PW_{12}O_{40}/Ta_2O_5–Si(Me/Ph)$, $H_3PW_{12}O_{40}–ZrO_2/Si(Et/Ph)Si$ or $H_3PW_{12}O_{40}–Ta_2O_5/Si(Et/Ph)Si$ with respect to alkyl-free $H_3PW_{12}O_{40}/ZrO_2$ or $H_3PW_{12}O_{40}/Ta_2O_5$ is due to the combination of increased surface hydrophobic character and excellent textural properties of the hybrid catalysts. The incorporation of alkyl groups-containing organosilica moieties within $H_3PW_{12}O_{40}/ZrO_2$ or $H_3PW_{12}O_{40}/Ta_2O_5$ framework selectively created an unsuitable environment for hydrophilic water or glycerol, leading to them easy desorption from the catalyst surface. Accordingly, the accessibility of active site center to the hydrophobic TG or FFA is increased, which facilitates the transesterification or esterification proceeding at a fast rate. At the same time, acid site

deactivation due to the strong adsorption of glycerol on the catalyst surface is inhibited, leading to the catalysts with excellent reusability. Additionally, incorporation of alkyl groups-containing organosilica moieties significantly improved the textural properties of $H_3PW_{12}O_{40}/ZrO_2$ or $H_3PW_{12}O_{40}/Ta_2O_5$, leading to 3D interconnected hybrid materials with large BET surface area and uniform pore size distribution, which give a positive contribution to the catalytic activity. For the $H_3PW_{12}O_{40}$–Ta_2O_5/Si(Et/Ph)Si or $H_3PW_{12}O_{40}$–ZrO_2/Si(Et/Ph)Si hybrid catalysts with much higher organic functionality content, although they exhibited perfect textural properties, their esterification or transesterification reactivity were lower than alkyl-free $H_3PW_{12}O_{40}/Ta_2O_5$ or $H_3PW_{12}O_{40}/ZrO_2$. This is due to the obvious loss of Ta_2O_5 or ZrO_2 sites in the hybrid catalysts, implying the catalytic activity of the prepared hybrid catalysts are mainly dominated by their strong Brønsted and Lewis acid properties.

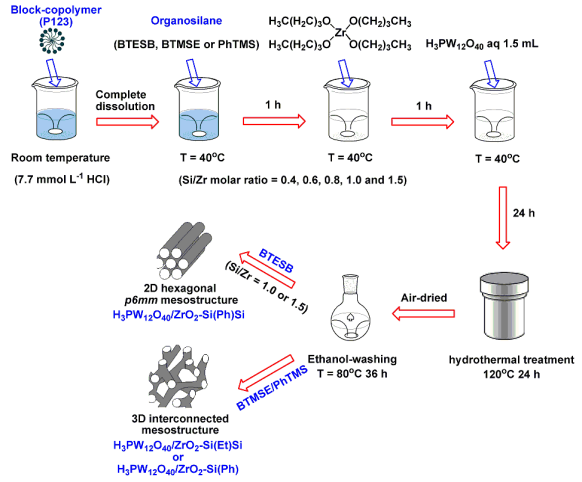

Fig. 13 Routes for the pore morphology-controlled preparation of mesostructured ZrO_2-based hybrid catalysts functionalized by both organosilica moieties and Keggin-type HPA. (Adapted from ref. 144)

Further research work focuses on the pore morphology-controlled preparation of ZrO_2-based hybrid catalysts functionalized by both hydrophobic alkyl groups (*i.e.* benzene-terminally bonded organosilica moieties and ethane- or benzene-bridged organosilica moieties) and Keggin-type HPA, $H_3PW_{12}O_{40}/ZrO_2$–Si(Ph) and $H_3PW_{12}O_{40}/ZrO_2$–Si(Et/Ph)Si, *via* one-pot P123-assisted sol–gel co-condensation–hydrothermal treatment procedure (Fig. 13), and then the relationships between the heterogeneous acid catalytic activity of HPA-based hybrid catalysts and the acidity, porosity and surface hydrophobicity/hydrophilicity were revealed by choosing the synthesis of levulinate esters from esterification of levulinic acid as the target reaction.[145,147]

It is an interesting challenge to prepare mesoporous HPA-based hybrid catalysts with controllable structural orderings and pore geometries by one step template-assisted sol–gel co-condensation route due to the complex preparation procedure and poor processability of HPA clusters. The circumstance is more difficult especially for selecting non-silica material such as ZrO_2,

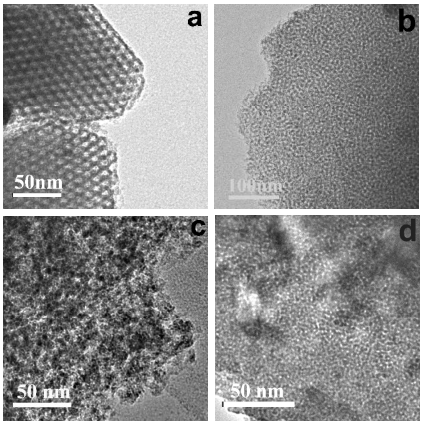

Fig. 14 TEM images of various ZrO_2-based hybrid catalysts. $H_3PW_{12}O_{40}/ZrO_2$–Si(Ph)Si-$2D_{hex}$ (a); $H_3PW_{12}O_{40}/ZrO_2$–Si(Ph)Si-$3D_{int}$ (b); $H_3PW_{12}O_{40}/ZrO_2$–Si(Et)Si-$3D_{int}$ (c) and $H_3PW_{12}O_{40}/ZrO_2$–Si(Ph)-$3D_{int}$ (d). (Adapted from ref. 144.)

Ta_2O_5, Nb_2O_5 or TiO_2 as the support. For example, $H_3PW_{12}O_{40}$ begins to decompose at pH higher than 1.5 and loses all acidic protons at 465 °C.[148,149] Therefore, creating mesostructured HPA-based hybrid catalysts should avoid decomposition of the HPA structure. Accordingly, acidity of the preparation system should be controlled at pH lower than 1.5 and boiling ethanol washing rather than high temperature calcination is selected to remove the nonionic surfactant. In addition, the heteropolyanions can perturb the self-assembly of organic and inorganic aggregates due to their strong complexation with nonionic surfactants, leading to long-range disordered mesostructures. As a consequence, the preparation conditions should be controlled carefully to create a suitable environment for self-assembling nonionic surfactant into a lyotropic liquid-crystalline phase at the beginning of mixing the surfactant, organic and inorganic precursors, which is the key step to fabrication of HPA-based hybrid catalysts with well-ordered mesostructure. Bearing these points in mind, by using different organosilica precursors (BTESB, BTMSE or PhTMS) and tuning the initial molar ratios of organosilica precursor to Zr source ($Zr(OC_4H_9)_4$), the prepared HPA-based hybrid catalysts exhibited different structural orderings and pore geometries. For the benzene-bridged hybrid materials prepared at initial Si/Zr molar ratio of 1.0 and 1.5, they show well-ordered 2D hexagonal *p6mm* mesostructure ($H_3PW_{12}O_{40}/ZrO_2$–Si(Ph)Si-$2D_{hex}$, Fig. 14a). As for the hybrid materials prepared at initial Si/Zr molar ratio lower than 1.0, they display disordered 3D interconnected mesostructure ($H_3PW_{12}O_{40}/ZrO_2$–Si(Ph)Si-$3D_{int}$, Fig. 14b). On the one hand, at the same initial Si/Zr molar ratio (*e.g.* 1.0), the pore morphologies of as-prepared HPA-based hybrid materials are dominated by the structures of organosilica precursors. For example, ethane-bridged or benzene-terminally bonded hybrid catalyst exhibited 3D interconnected porous channel ($H_3PW_{12}O_{40}/ZrO_2$–Si(Et)Si-$3D_{int}$ and $H_3PW_{12}O_{40}/ZrO_2$–$Si(Ph)_{int}$ in Fig. 14c and d). For alkyl-bridged $H_3PW_{12}O_{40}/ZrO_2$–Si(R)Si (R = $–CH_2CH_2–$ or $–C_6H_4–$) materials, the $O_{1.5}$–Si–C–Si–$O_{1.5}$ fragments as bridging components are introduced into ZrO_2 framework through –Zr–O–Si–C–Si–O– linkages. The rigid construction of $–C_6H_4–$ group is responsible for the retention of the ordered mesostructure after P123 removing, while the

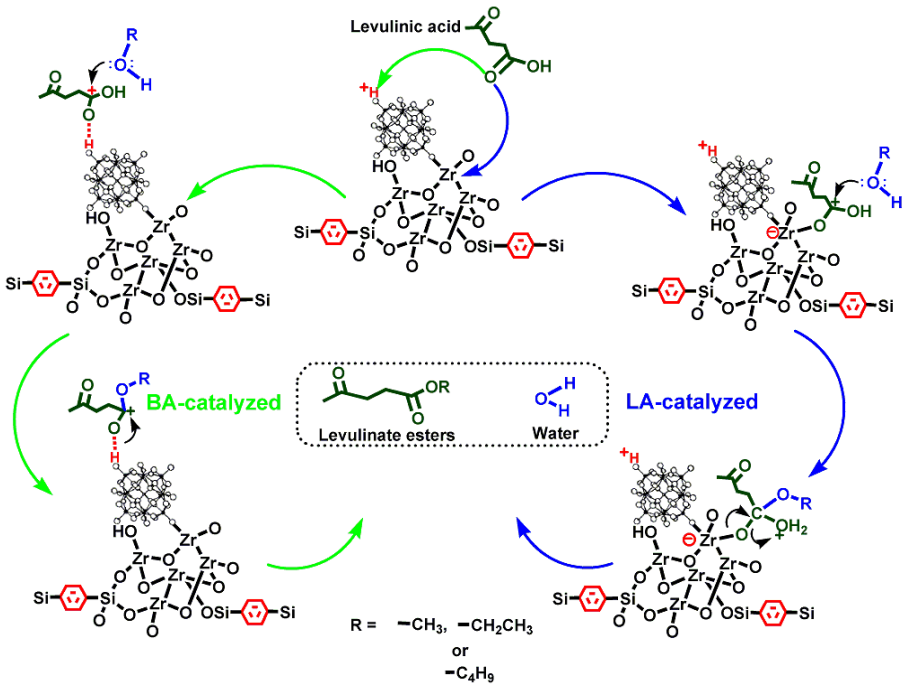

Fig. 15 Process of esterification of levulinic acid with alcohol to produce levulinate esters catalyzed over the $H_3PW_{12}O_{40}/ZrO_2$–Si(Ph)Si hybrid materials. Left part: Brønsted acid site-catalyzed reaction; right part: Lewis acid site-catalyzed reaction. (Adapted from ref. 144.)

flexibility of the $–CH_2CH_2–$ group leads to the construction distortion and thereby the disordered mesostructure of the $H_3PW_{12}O_{40}/ZrO_2$–Si(Et)Si-$3D_{int}$ after removing P123. As for the benzene-terminally bonded $H_3PW_{12}O_{40}/ZrO_2$–Si(Ph)-$3D_{int}$, the phenyl groups position in the pore channel rather than pore wall of the hybrid catalyst, which lead to the catalyst insufficient structural rigidity to form the ordered mesostructure after P123 removal. The studies confirm that bissilylated organic precursor BTESB is an excellent structural ordering adjusting agent, and suitable amount of BTESB can ensure the hybrid materials with highly ordered mesostructure.

Compared with alkyl-free $H_3PW_{12}O_{40}/ZrO_2$, $H_3PW_{12}O_{40}/ZrO_2$–Si(Et/Ph)Si or $H_3PW_{12}O_{40}/ZrO_2$–Si(Ph) hybrid catalyst exhibits obviously enhanced heterogeneous acid catalytic activity towards the synthesis of levulinate esters including methyl, ethyl and *n*-butyl levulinate from biomass-derived platform molecule, levulinic acid, under atmospheric pressure refluxing conditions, regardless of their pore morphologies (Table 6). For example, after the reaction proceeded for 2 h, the yield of methyl levulinate reached 45.1, 58.3, 89.9 and 59.4%, respectively, for $H_3PW_{12}O_{40}/ZrO_2$-, $H_3PW_{12}O_{40}/ZrO_2$–Si(Et)Si-$3D_{int}$-, $H_3PW_{12}O_{40}/ZrO_2$–Si(Ph)Si-$2D_{hex}$- and $H_3PW_{12}O_{40}/ZrO_2$–Si(Ph)-$3D_{int}$-catalyzed esterification reaction. This excellent acid catalytic activity originates from the combination of strong Brønsted as well as Lewis acidity of the $H_3PW_{12}O_{40}/ZrO_2$ (Fig. 15), rationally designed porosity and the enhanced surface hydrophobicity of the hybrid catalysts. Moreover, ordered 2D hexagonal mesostructured $H_3PW_{12}O_{40}/ZrO_2$–Si(Ph)Si-$2D_{hex}$ exhibited much higher catalytic activity with respect to 3D interconnected wormhole-like $H_3PW_{12}O_{40}/ZrO_2$–Si(Et)Si-$3D_{int}$ or $H_3PW_{12}O_{40}/ZrO_2$–Si(Ph)-$3D_{int}$, attributed to the decreased mass transfer limitations of the reactants and products owing to the ordered mesoporous structure. Additionally, by-products such as dialkyl ethers due to etherification reactions under higher temperature were hardly found in current reaction system.

One of the most important factors of heterogeneous catalysts contributing to catalytic performance is the stability against leaching of the active sites during reactions. The recyclability of the above HPA-based hybrid catalysts including $H_3PW_{12}O_{40}/ZrO_2(Ta_2O_5)$, $H_3PW_{12}O_{40}/ZrO_2(Ta_2O_5)$–Si(Ph/Et)Si and $H_3PW_{12}O_{40}/ZrO_2(Ta_2O_5)$–Si(Ph/Me) were evaluated, and it showed the hybrid catalyst can be used at least three times without significant loss of reactivity, and leaching of the Keggin unit into the reaction media was hardly found. Therefore, they performed as genuine heterogeneous acid catalysts in both esterification and transesterification, exhibiting potential in practical applications. This excellent catalytic stability is due to the strong covalent interaction between the Keggin units and ZrO_2 (or Ta_2O_5) support as well as the enhanced surface hydrophobicity.

However, it should admit that the aforementioned hybrid acid catalysts-catalyzed transesterification reactions, although carried out at atmosphere refluxing temperature of alcohol, were done with a large excess of alcohol to obtain considerably fast reaction rate. Therefore, design of more robust solid acid catalysts for biodiesel production under mild conditions is still a challenge. Additionally, the research work should be continued to evaluate the possibility of using as-prepared HPA-based hybrid catalysts for an industrial biodiesel production starting from crude oils in the presence of various impurities such as salt, water and FFAs. Current research indicated that transesterification of waste cooling oil and inedible virgin plant oils such as *ESG* seed oil and *Xanthoceras sorbifolia* Bunge seed oil catalyzed by HPA-based

hybrid catalysts showed considerably high FAME yields; meanwhile, the catalysts can be reused 3–5 times without significant activity loss. More extensive research on this tropic including mechanical properties of the catalysts is underway to find out the feasibility of as-prepared hybrid solid catalysts for industrial biodiesel production.

4. Conclusion and Outlook

The use of solid acids for "*second generation*" biodiesel production from waste or low-grade oils is an emerging research field since recent studies have proved the technical feasibility and the environmental and economical benefits of heterogeneous acid-catalyzed esterification and transesterification. Numerous solid acids such as sulfated metal oxides, H-form zeolites, sulfonic ion-exchange resins, sulfonic modified mesostructured silica materials, sulfonated carbon-based catalysts, heteropolyacids, ZrO_2- or Ta_2O_5-supported heteropolyacids and acidic ionic liquids have been extensively studied for this topic. However, although these solid acids show acceptable reactivity towards esterification of long chain FFAs, their reactivity to the transesterification of viscous TGs-containing oily feedstocks is generally unsatisfactory. Therefore, most of the aforementioned solid acid-catalyzed transesterification reactions proceed under stringent conditions including higher temperature, higher pressure, an excess of alcohol as well as longer reaction time, which are not favorable for industrial applications. Moreover, solid acid catalysts often suffer from problems of deactivation, poisoning and acid site leaching in the reaction medium. Thereby, design of efficient, robust and catalytically stable solid acid catalysts that can improve the overall efficiency of biodiesel production dramatically is still an important challenge. To meet this challenge, the following two important strategies should be considered. Firstly, tuning the porosity and surface hydrophilic/hydrophobic balance of the solid acids so that mass-transport can be enhanced and diffusional limitation, catalyst deactivation and poisoning are avoided. Excellent porosity includes uniform pore channel, large pore diameter, large surface area as well as high pore volume can increase acid site population and the accessibility of acid site on a given catalysts surface and inside the pores to the substrates as well as decrease the mass-transport limitation of the reactant or product molecules, while hydrophobic surface can promote the preferential adsorption of oily hydrophobic species on the solid acid surface and avoid possible deactivation of acid sites by strong adsorption of polar compounds such as glycerol and water. On the other hand, careful design one step catalyst preparation route avoiding multistep grafting method so that the interaction between the acid sites and the catalyst framework structure can be strengthened, and thereby leakage of the active phases is inhibited. To meet the requirement of both of points, one step template-assisted sol–gel co-condensation route is designed, and tuning the porosity and surface hydrophobic/hydrophilic balance of the solid acids can be realized simultaneously by the incorporation of hydrophobic alkyl groups-containing organosilica moieties into the framework structure of solid acids including SO_4^{2-}/ZrO_2, $H_3PW_{12}O_{40}/Ta_2O_5$ and $H_3PW_{12}O_{40}/ZrO_2$. By the combination of strong acidity, well-defined mesoporosity and increased surface hydrophobicity, the designed organic-inorganic hybrid catalysts such as SO_4^{2-}/ZrO_2–SiO_2(Et/Ph), $H_3PW_{12}O_{40}$–ZrO_2/Si(Et/Ph)Si, $H_3PW_{12}O_{40}$–Ta_2O_5/Si(Et/Ph)Si, $H_3PW_{12}O_{40}/ZrO_2$–Si(Me/Ph) and $H_3PW_{12}O_{40}/Ta_2O_5$–Si(Me/Ph) exhibited excellent catalytic activity in both esterification and transesterification reactions at atmosphere refluxing temperature of alcohol. Meanwhile, the acid site deactivation due to the strong adsorption of water or glycerol on the catalyst surface as well as acid site leaching in the reaction medium is inhibited, resulting in the hybrid catalysts good catalytic stability; moreover, the regeneration of the catalysts can be realized by washing with dichloromethane rather than commonly used thermal treatments, accordingly, structure integrities of SO_4^{2-}/ZrO_2, the Keggin unit and organic functionalities can be preserved. Additionally, structural orderings and pore geometries controlled fabrication of mesostructured SO_4^{2-}/ZrO_2–SiO_2(Et/Ph) or $H_3PW_{12}O_{40}$–ZrO_2/Si(Et/Ph)Si hybrid catalysts with 2D hexagonal *p6mm*, 3D cubic *Im3m* and 3D interconnected wormhole-like pore morphologies are successfully realized by selecting different organicsilica precursors and adjusting suitable Si/Zr molar ratios, types of surfactants and the preparation conditions. The present research result showed that the hybrid catalysts with 2D hexagonal *p6mm* mesostructure exhibited the highest catalytic activity towards both esterification and transesterification reactions among the above hybrid catalysts with various pore morphologies. This enhanced catalytic activity is due to the fact that the ordered mesostructure can decrease mass-transport limitation of the reactants and products significantly. However, owing to the complexity of the porous hybrid acid catalysts and the catalytic processes, this research topic should be carried out thoroughly, which is important to guide the rational design of novel solid acids for biodiesel production.

We thank the Natural Science Fund Council of China (21173036; 51278092) for financial support.

Notes and references

School of Chemistry, Northeast Normal University, Changchun 130024, P.R. China. Tel./fax: +86 431 85098705. E-mail: guoyh@nenu.edu.cn (Y. Guo)

1 R. Luque, J. C. Lovett, B. Datta, J. Clancy, J. M. Campelo and A. A. Romero, *Energy Environ. Sci*., 2010, **3**, 1706–1721.
2 K. Wilson and A. F. Lee, *Catal. Sci. Technol*., 2012, **2**, 884–897.
3 Y. B. Huang and Y. Fu, *Green Chem*., 2013, **15**, 1095–1111.
4 M. D. Serio, M. Cozzolino, M. Giordano, R. Tesser, P. Patrono and E. Santacesaria, *Ind. Eng. Chem. Res.*, 2007, **46**, 6379–6384.
5 M. D. Serio, R. Tesser, L. Pengmei and E. Santacesaria, *Energy Fuels*, 2008, **22**, 207–217.
6 M. K. Lam, K. T. Lee and A. R. Mohamed, *Biotechnol. Adv.*, 2010, **28**, 500–518.
7 Y. C. Sharma, B. Singh and J. Korstad, *Biofuels, Bioprod. Bioref.*, 2011, **5**, 69–92.
8 S. Al-Zuhair, *Biofuels, Bioprod. Bioref.*, 2007, **1**, 57–66.
9 B. Walter, J. F. Gruson and G. Monnier, *Oil & Gas Science and Technology-Revue De L Institut Francais Du Petrole*, 2008, **63**, 387–393.
10 *International Energy Agency I. Key world energy statistic*, 2006.
11 *International Energy Agency I. Key world energy statistic*, 2008.
12 M. Mittelbach, C. Remschmidt and Boersedruck Ges.m.b.H, *Biodiesel, the comprehensive handbook*, 2nd edn, Vienna, Graz, Austria, 2004.
13 A. Demirbas, *Energy Convers. Manage.*, 2009, **50**, 14–34.
14 A. K. Agarwal and L. M. Das, *Trans. ASME*, 2001, **123**, 440–447.
15 E. Lotero, Y. Liu, D. E. Lopez, K. Suwannakarn, D. A. Bruce and J. G. Goodwin, Jr., *Ind. Eng. Chem. Res.*, 2005, **44**, 5353–5363.

16 A. A. Kiss, A. C. Dimian and G. Rothenberg, *Adv. Synth. Catal.*, 2006, **348**, 75–81.
17 L. Bournay, D. Casanave, B. Delfort, G. Hillion and J. A. Chodorge, *Catal. Today*, 2005, **106**, 190–192.
18 A. J. Kinney and T. E. Clemente, *Fuel Process. Technol.*, 2005, **86**, 1137–1147.
19 M. L. Granados, M. D. Zafra Poves, D. M. Alonso, R. Mariscal, F. C. Galisteo, R. Moreno-Tost, J. Santamaría and J. L. G. Fierro, *Appl. Catal., B*, 2007, **73**, 317–326.
20 P. Felizardo, M. J. Neiva Correia, I. Raposo, J. F. Mendes, R. Berkemeier and J. M. Bordado, *Waste Manage.*, 2006, **26**, 487–494.
21 M. G. Kulkarni and A. K. Dalai, *Ind. Eng. Chem. Res.*, 2006, **45**, 2901–2913.
22 Y. Wang, S. Ou, P. Liu, F. Xue and S. Tang, *J. Mol. Catal. A,* 2006, **252**, 107–112.
23 G. J. Suppes, M. A. Dasari, E. J. Doskocil, P. J. Mankidy and M. J. Goff, *Appl. Catal., A*, 2004, **257**, 213–223.
24 H. Fukuda, A. Kondo and H. Noda, *J. Biosci. Bioeng.*, 2001, **92**, 405–416.
25 C. R. V. Reddy, R. Oshel and J. G. Verkade, *Energy Fuels*, 2006, **20**, 1310–1314.
26 W. L. Xie and X. M. Huang, *Catal. Lett.*, 2006, **107**, 53–59.
27 G. Arzamendi, I. Campo, E. Arguiñarena, M. Sánchez, M. Montes and L. M. Gandía, *Chem. Eng. J.*, 2007, **134**, 123–130.
28 H. J. Kim, B. S. Kang, M. J. Kim, Y. M. Park, D. K. Kim, J. S. Lee and K. Y. Lee, *Catal. Today*, 2004, **93**, 315–320.
29 T. Ebiura, T. Echizen, A. Ishikawa, K. Murai and T. Baba, *Appl. Catal. A*, 2005, **283**, 111–116.
30 D. Y. C. Leung, X. Wu and M. K. H. Leung, *Appl. Energy*, 2010, **87**, 1083–1095.
31 K. Faungnawakij, B. Yoosuk, S. Namuangruk, P. Krasae, N. Viriya-empikul and B. Puttasawat, *ChemCatChem*, 2012, **4**, 209–216.
32 M. Hara, *Energy Environ. Sci.*, 2010, **3**, 601–607.
33 S. Zheng, M. Kates, M. A. Dubé, D. D. McLean, *Biomass Bioenerg.*, 2006, **30**, 267–272.
34 B. Freedman, E. H. Pryde, T. L. Mounts, *J. Am. Oil Chem. Soc.*, 1984, **61**, 1638–1643.
35 K. Jacobson, R. Gopinath, L. C. Meher, A. K. Dalai, *Appl. Catal. B*, 2008, **85**, 86–91.
36 C. Descorme, P. Gallezot, C. Geantet and C. George, *ChemCatChem*, 2012, **4**, 1897–1906.
37 A. Sivasamy, K. Y. Cheah, P. Fornasiero, F. Kemausuor, S. Zinoviev, S. Miertus, *ChemSusChem*, 2009, **2**, 278–300.
38 A. C. Pinto, L. L. N. Guarieiro, M. J. C. Rezende, N. M. Ribeiro, E. A. Torres, W. A. Lopes, P. A. P. Pereira and J. B. de Andrade, *J. Braz. Chem. Soc*., 2005, **16**, 1313–1330.
39 R. Rinaldi and F. Schüth, *Energy Environ. Sci*., 2009, **2**, 610–626.
40 E. Santacesaria, G. M. Vicenteb, M. D. Serioa and R. Tesser, *Catal. Today*, 2012, **195**, 2–13.
41 K. Arata, *Green Chem.*, 2009, **11**, 1719–1728.
42 B. M. Reddy and M. K. Patil, *Chem. Rev.*, 2009, **109**, 2185–2208.
43 X. R. Chen, Y. H. Ju and C. Y. Mou, *J. Phys. Chem. C*, 2007, **111**, 18731–18737.
44 D. Rattanaphra, A. P. Harvey, A. Thanapimmetha, P. Srinophakun, *Renew. Energy*, 2011, **36**, 2679–2686.
45 A. M. Alsalme, P. V. Wiper, Y. Z. Khimyak, E. F. Kozhevnikova and I. V. Kozhevikov, *J. Catal.*, 2010, **276**, 181–189.
46 T. Jin, T. Yamaguchi and K. Tanabe, *J. Phys. Chem.*, 1986, **90**, 4794–4796.
47 W. Li, F. Y. Ma, F. Su, L. Ma, S. Q. Zhang and Y. H. Guo, *ChemSusChem,* 2011, **4**, 744–756.
48 J. A. Melero, J. Igesias and G. Morales, *Green Chem.*, 2009, **11**, 1285–1308.
49 K. Suwannakarn, E. Lotero, J. G. Goodwin Jr. and C. Q. Lu, *J. Catal.*, 2008, **255**, 279–286.
50 J. Ni and F. C. Meunier, *Appl. Catal. A*, 2007, **333**, 122–130.
51 Y. M. Park, J. Y. Lee, S. H. Chung, I. S. Park, S. Y. Lee, D. K. Kim and K. Y. Lee, *Bioresour. Technol.*, 2010, **101**, S59–S61.
52 A. Corma, *Chem. Rev.*, 1995, **95**, 559–614.
53 G. D. Yadav and J. J. Nair, *Micropor. Mesopor. Mater.*, 1999, **33**, 1–48.
54 I. Jiménez-Morales, J. Santamaría-González, P. Maireles-Torres and A. Jiménez-López, *Appl. Catal. B*, 2011, **103**, 91–98.
55 T. A. Peters, N. E. Benes, A. Holmen and J. T. F. Keurentjes, *Appl. Catal. A*, 2006, **297**, 182–188.
56 J. Y. Park, Z. M. Wang, D. K. Kim and J. S. Lee, *Renew. Energy*, 2010, **35**, 614–618.
57 Y. J. Liu, E. Lotero and J. G. Goodwin Jr., *J. Catal.*, 2006, **242**, 278–286.
58 Y. J. Liu, E. Lotero and J. G. Goodwin Jr., *J. Catal.*, 2006, **243**, 221–228.
59 L. Guerreiro, J. E. Castanheiro, I. M. Fonseca, R. M. M. Aranda, A. M. Ramos and J. Vital, *Catal. Today*, 2006, **118**, 166–171.
60 D. E. López, J. G. Goodwin Jr., D. A. Bruce and E. Lotero, *Appl. Catal. A*, 2005, **295**, 97–105.
61 D. E. López, J. G. Goodwin Jr. and D. A. Bruce, *J. Catal.*, 2007, **245**, 381–391.
62 B. M. E. Russbueldt and W. F. Hoelderich, *Appl. Catal. A*, 2009, **362**, 47–57.
63 R. Tesser, L. Casale, D. Verde, M. D. Serio and E. Santacesaria, *Chem. Eng. J.*, 2010, **157**, 539–550.
64 E. Andrijanto, E. A. Dawsona and D. R. Brown, *Appl. Catal. B*, 2012, **115–116**, 261–268.
65 Y. Liu and L. Wang, *Chem. Technol. Fules Oils*, 2009, **45**, 417–424.
66 D. Zuo, J. Lane, D. Culy, M. Schultz, A. Pullar and M. Waxman, *Appl. Catal. B*, 2013, **129**, 342**–**350.
67 C. Pirez, J. M. Caderon, J. P. Dacquin, A. F. Lee and K. Wilson, *ACS Catal*., 2012, **2**, 1607−1614.
68 I. Mbaraka, B. H. Shanks, *J. Catal.* ,2005, **229**, 365–373
69 J. Dhainaut, J. P. Dacquin, A. F. Lee and K. Wilson, *Green Chem*., 2010, **12**, 296–303.
70 J. J. Woodford, J. P. Dacquin, K. Wilson and A. F. Lee, *Energy Environ. Sci*., 2012, **5**, 6145−6150.
71 M. H. Tucker, A. J. Crisci, B. N. Wigington, N. Phadke, R. Alamillo, J. Zhang, S. L. Scott and J. A. Dumesic, *ACS Catal.*, 2012, **2**, 1865−1876.
72 F. Hoffmann, M. Cornelius, J. Morell and M. Fröba, *Angew. Chem. Int. Ed.*, 2006, **45**, 3216−3251.
73 M. Hara, T. Yoshida, A. Takagaki, T. Takata, J. N. Kondo, K. Domen and S. Hayashi, *Angew. Chem. Int. Ed.*, 2004, **43**, 2955–2958.
74 M. H. Zong, Z. Q. Duan, W. Y. Lou, T. J. Smith, H. Wu, *Green Chem.*, 2007, **9**, 434–437.
75 W. Y. Lou, M. H. Zong and Z. Q. Duan, *Bioresour. Technol.*, 2008, **99**, 8752–8758.
76 S. Suganuma, K. Nakajima, M. Kitano, D. Yamaguchi, H. Kato, S. Hayashi and M. Hara, *J. Am. Chem. Soc.*, 2008, **130**, 12787–12793.
77 M. Okamura, A. Takagaki, M. Toda, J. N. Kondo, T. Tatsumi, K. Domen, M. Hara and S. Hayashi, *Chem. Mater.*, 2006, **18**, 3039–3045.
78 K. Nakajima and M. Hara, *ACS Catal.*, 2012, **2**, 1296–1304.
79 P. F. Siril, H. E. Cross and D. R. Brown, *J. Mol. Catal. A*, 2008, **279**, 63–68.
80 M. Kitano, D. Yamaguchi, S. Suganuma, K. Nakajima, H. Kato, S. Hayashi and M. Hara, *Langmuir*, 2009, **25**, 5068–5075.
81 J. A. Maciá-Agulló, M. Sevilla, M. A. Diez and A. B. Fuertes, *ChemSusChem*, 2010, **3**, 1352–1354.
82 B. Chang, J. Fu, Y. Tian and X. Dong, *J. Phys. Chem. C*, 2013, **117**, 6252−6258.
83 Q. Shu, J. X. Gao, Z. Nawaz, Y. H. Liao, D. Z. Wang and J. F. Wang, *Appl. Energy*, 2010, **87**, 2589−2596.
84 Q. Shu, Z. Nawaz, J. X. Gao, Y. H. Liao, Q. Zhang, D. Z. Wang, J. F. Wang, *Bioresour. Technol.*, 2010, **101**, 5374−5384.
85 M. T. Pope and A. Müller, *Angew. Chem. Int. Ed. Engl.*, 1991, **30**, 34–48.
86 M. Mizuno and M. Misono, *Chem. Rev.*, 1998, **98**, 199–217.
87 M. Misono, *Chem. Commun.*, 2001, 1141–1152.
88 I. V. Kozhevnikov, *Chem. Rev.*, 1998, **98**, 171–198.
89 T. Okuhara, *Chem. Rev.*, 2002, **102**, 3641–3666.
90 E. Grinenval, X. Rozanska, A. Baudouin, E. Berrier, F. Delbecq, P. Sautet, J. M. Basset and F. Lefebvre, *J. Phys. Chem. C*, 2010, **114**, 19024–19034.
91 I. Noshadi, N. A. S. Amin and R. S. Pamas, *Fuel*, 2012, **94**, 156–164.

92 P. Morin, B. Hamad, G. Sapaly, M. G. C. Rocha, P. G. P. de Oliveira, W. A. Gonzalez, E. A. Sales and N. Essayem, *Appl. Catal. A*, 2007, **330**, 69–76.

93 F. H. Cao, Y. Chen, F. Y. Zhai, J. Li, J. H. Wang, X. H. Wang, S. T. Wang and W. M. Zhu, *Biotechnol. Bioeng.*, 2008, **101**, 93–100.

94 X. D. Yu, Y. H. Guo, K. X. Li, X. Yang, L. L. Xu, Y. N. Guo and J. L. Hu, *J. Mol. Catal. A*, 2008, **290**, 44–53.

95 K. Narasimharao, D. R. Brown, A. F. Lee, A. D. Newman, P. F. Siril, S. J. Tavener and K. Wilson, *J. Catal.*, 2007, **248**, 226–234.

96 C. Baroi and A. K. Dalai, *Catal. Today*, 2013, **207**, 74–85.

97 V. Brahmkhatri and A. Patel, *Fuel*, 2012, **102**, 72–77.

98 V. Brahmkhatri and A. Patel, *Appl. Catal. A*, 2011, **403**, 161–172.

99 M. G. Kulkarni, R. Gopinath, L. C. Meher and A. K. Dalai, *Green Chem.*, 2006, **8**, 1056–1062.

100 A. Alsalme, E. F. Kozhevnikova and I. V. Kozhevnikov, *Appl. Catal. A*, 2008, **349**, 170–176.

101 K. Srilatha, T. Issariyakul, N. Lingaiah, P. S. Sai Prasad, J. Kozinski and A. K. Dalai, *Energy Fuel*, 2010, **24**, 4748–4755.

102 K. Srilatha, N. Lingaiah, B. L. A. Peabharathi Devi, R. B. N. Prasad, S. Venkateswar and P. S. Sai Prasad, *Appl. Catal. A*, 2009, **365**, 28–33.

103 C. F. Oliveira, L. M. Dezaneti, F. A. C. Garcia, J. L. De Macedo and J. A. Dias, *Appl. Catal. A*, 2010, **372**, 153–161.

104 A. S. Badday, A. Z. Abdullah and K. T. Lee, *Renew. Energy*, 2014, **62**, 10–17.

105 G. S. Armatas, G. Bilis and M. Louloudi, *J. Mater. Chem.*, 2011, **21**, 2997–3005.

106 J. Alcañiz-Monge, G. Trautwein, J. P. Marco-Lozar, *Appl. Catal. A*, 2013, **468**, 432– 441.

107 V. Brahmkhatri, A. Patel, *Appl. Catal. A*, 2011, **403**, 161–172.

108 A. Patel, N. Narkhede, Energy Fuels, 2012, **26**, 6025–6032.

109 C. F. Oliveira, L. M. Dezaneti, F. A.C. Garcia, J. L. de Macedo, J. A. Dias, S. C.L. Dias, K. S.P. Alvim, 2010, **372**, 153–161.

110 J. H. Clark, D. J. Macquarrie and S. J. Tavener, *Dalton Trans.*, 2006, 4297–4309.

111 T. L., Greaves and C. J. Drummond, *Chem. Rev.*, 2008, **108**, 206–237.

112 A. Kamal and G. Chouhan, *Adv. Synth. Catal.*, 2004, **346**, 579–582.

113 X. Z. Liang and J. Q. Yang, *Green Chem.*, 2010, **12**, 201–204.

114 X. Z. Liang, *Ind. Eng. Chem. Res*., 2013, **52**, 6894−6900.

115 M. Ghiaci, B. Aghabarari, S. Habibollahi and A. Gil, *Bioresour. Technol.*, 2011, **102**, 1200−1204.

116 L. Zhang, M. Xian, Y. He, L. Li, J. Yang, S. Yu, X. Xu, *Bioresour. Technol.*, 2009, **100**, 4368−4373.

117 X. M. Liu, Z. X. Song and H. J. Wang, *Struct. Chem.*, 2009, **20**, 509−515.

118 Q. Wu, H. Chen, M. H. Han, D. Z. Wang and J. F. Wang, Ind. Eng. Chem. Res., 2007, **46**, 7955–7960.

119 J. M. Miao, H. Wan, Y. B. Shao, G. F. Guan and B. Xu, *J. Mol. Catal. A*, 2011, **348**, 77−82.

120 Z. J. Xu, H. Wan, J. M. Miao, M. J. Han, C. Y ang and G. F. Guan, *J. Mol. Catal. A*, 2010, **332**, 152−157.

121 B. Karimi and M. Vafaeezadeh, *Chem. Commun.*, 2012, **48**, 3327–3329.

122 B. Zhen, H. S. Li, Q. Z. Jiao, Y. Li, Q. Wu and Y. P. Zhang, *Ind. Eng. Chem. Res.*, 2012, **51**, 10374−10380.

123 F. J. Liu, L. Wang, Q. Sun, L. F. Zhu, X. J. Meng and F. S. Xiao, *J. Am. Chem. Soc.*, 2012, **134**, 16948−16950.

124 Y. Leng, J. Wang, D. R. Zhu, X. Q. Ren, H. Q. Ge and L. Shen, *Angew. Chem. Int. Ed.*, 2009, **121**, 174 –177.

125 A. Taguchi and F. Schüth, *Micropor. Mesopor. Mater*., 2005, **77**, 1–45.

126 F. Goettmann and C. Sanchez, *J. Mater. Chem*., 2007, **17**, 24–30.

127 W. Schmidt, *ChemCatChem*, 2009, **1**, 53−67.

128 M. Stöcker, *Angew. Chem. Int. Ed*., 2008, **47**, 9200–9211.

129 Y. Wan and D. Y. Zhao, *Chem. Rev*., 2007, **107**, 2821−2860.

130 G. S. Armatas, A. P. Katsoulidis, D. E. Petrakisc and P. J. Pomonis, *J. Mater. Chem*., 2010, **20**, 8631–8638.

131 E. Serrano, N. Linares, J. Garcia-Martinez and J. R. Berenguer, *ChemCatChem*, 2013, **5**, 844–860.

132 A. Bail, V. C. Santosa, M. R. Freitas, L. P. Ramosb, W. H. Schreiner, G. P. Ricci, K. J. Ciuffi and S. Nakagaki, *Appl. Catal. B*, 2013, **130**–**131**, 314–324.

133 K. X. Li, J. L. Hu, W. Li, F. Y. Ma, L. L. Xu and Y. H. Guo, *J. Mater. Chem*., 2009, **19**, 8628–8638.

134 P. Vazquez, L. Pizzio, G. Romanelli, J. Autino, C. Caceres and M. Blanco, *Appl. Catal*. *A*, 2002, **235**, 233–240.

135 B. Samaranch, P. R. Piscina, G. Clet, M. Houalla, P. Gélin and N. Homs, *Chem. Mater.*, 2007, **19**, 1445−1451.

136 T. Ushikubo and K. Wada, *Appl. Catal.*, 1990, **67**, 25–38.

137 B. M. Devassy and S. B. Halligudi, *J. Catal.*, 2005, **236**, 313–323.

138 L. L. Xu, Y. H. Wang, X. Yang, X. D. Yu and Y. H. Guo, J. H. Clark, *Green Chem.*, 2008, **10**, 746–755.

139 R. Sánchez-Vázquez, C. Pirez, J. Iglesias, K. Wilson, A. F. Lee, and J. A. Melero*, ChemCatChem*., 2013, **5**, 994–1001.

140 W. Li, Z. J. Jiang, F. Y. Ma, F. Su, L. Chen, S. Q. Zhang and Y. H. Guo, *Green Chem*., 2010, **12**, 2135–2138.

141 W. Li, F. Y. Ma, F. Su, L. Ma, S. Q. Zhang and Y. H. Guo, *ChemCatChem*, 2012, **4**, 1798–1807.

142 L. L. Xu, Y. H. Wang, X. Yang, J. L. Hu, W. Li and Y. H. Guo, *Green Chem.*, 2009, **11**, 314–317.

143 L. L. Xu, W. Li, J. L. Hu, X. Yang and Y. H. Guo, *Appl. Catal. B*, 2009, **90**, 587–594.

144 F. Su, Q. Y. Wu, D. Y. Song, X. H. Zhang, M. Wang and Y. H. Guo, *J. Mater. Chem. A*, 2013, **1**, 13209–13221.

145 L. L. Xu, W. Li, J. L. Hu, K. X. Li, X. Yang, F. Y. Ma, Y. N. Guo, X. D. Yu and Y. H. Guo, *J. Mater. Chem.*, 2009, **19**, 8571–8579.

146 F. Su, L. Ma, Y. H. Guo and W. Li, *Catal. Sci. Technol.*, 2012, **2**, 2367–2374.

147 F. Su, L. Ma, D. Y. Song, X. H. Zhang and Y. H. Guo, *Green Chem.*, 2013, **15**, 885–890.

148 Y. H. Guo, K. X. Li and J. H. Clark, *Green Chem*., 2007, **9**, 839–841.

149 Y. H. Guo, K. X. Li, X. D. Yu and J. H. Clark, *Appl. Catal. B*, 2008, **81**, 182–191.

150 I. Noshadi, N.A.S. Amin, R. S. Parnas, Fuel, 2012, 94, 156–164.